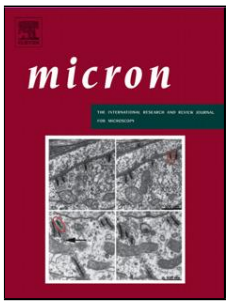

Title: The haemocytes of the colonial aplousobranch ascidian *Diplosoma listerianum*: structural, cytochemical and functional analyses

Authors: Francesca Cima, Anna Peronato, Loriano Ballarin

PII: S0968-4328(17)30271-8
DOI: http://dx.doi.org/10.1016/j.micron.2017.08.007
Reference: JMIC 2470

To appear in: *Micron*

Received date: 6-7-2017
Revised date: 22-8-2017
Accepted date: 23-8-2017

Please cite this article as: Cima, Francesca, Peronato, Anna, Ballarin, Loriano, The haemocytes of the colonial aplousobranch ascidian Diplosoma listerianum: structural, cytochemical and functional analyses.Micron http://dx.doi.org/10.1016/j.micron.2017.08.007

Title: The haemocytes of the colonial aplousobranch ascidian *Diplosoma listerianum*: structural, cytochemical and functional analyses
Running title: *Diplosoma* haemocytes

Authors: Francesca Cima, Anna Peronato, Loriano Ballarin

Affiliation: Department of Biology, University of Padova

Corresponding author:
Francesca Cima, Department of Biology, University of Padova
Via Ugo Bassi 58/B, 35121 Padova, Italy
Tel: +39 049 8276198; fax: +39 049 8276199
Email: francesca.cima@unipd.it

ORCID (Francesca Cima): 0000-0001-5232-3918
ORCID (Loriano Ballarin): 0000-0002-3287-8550

Highlights

- This is the first characterisation of haemocytes in an aplousobranch ascidian
- A series of microscopic techniques modified for invertebrate tissues is presented
- Behaviour and changes of haemocytes have been observed after experimental stimuli
- Eight morphotypes are described at both light and electron microscopy
- A comparative analysis with haemocytes of other ascidian orders is discussed

Abstract

Diplosoma listerianum is a colonial aplousobranch ascidian of the family Didemnidae that is native to the northeast Atlantic and exhibits a cosmopolitan distribution in temperate waters. It lacks a shared colonial circulation crossing the tunic, and the zooids are connected only by the common tunic. In the present study, the haemocytes of this ascidian were analysed via light and electron microscopy. Their phagocytic and enzymatic activities, staining and immunostaining properties, and lectin affinity were examined with

various classical methods reconsidered and modified for small marine invertebrates. Eight morphotypes were identified in reference to corresponding cell types described in other ascidians: undifferentiated cells (haemoblasts), storage cells for nitrogenous catabolites (nephrocytes) and immunocytes. The immunocytes are involved in immune responses, acting as (1) phagocytes, rich in hydrolases and involved in the clearance of both foreign particles and effete cells (hyaline amoebocytes and macrophage-like cells); (2) cytotoxic cells, able to degranulate and induce cytotoxicity through the release of the enzyme phenoloxidase after an immune stimulus (granular amoebocytes and morula cells); and (3) basophilic cells with an affinity for ConA and NPA that contain heparin and histamine and that show sensitivity to the compound 48/80, promoting their degranulation (mast cell-like granulocytes). In addition, a particular cell type showing exceptional development of the Golgi apparatus and large vacuoles containing a filamentous material has been recognised (spherule cell), for which a role in tunic repair and fibrogenesis has been hypothesised.

Keywords

Ascidians, cell degranulation, *Diplosoma listerianum*, enzyme histochemistry, haemocytes, immunohistochemistry, lectin affinity, phagocytosis, ultrastructure

1. Introduction

Ascidians are members of the Tunicata, the sister taxon of vertebrates (Delsuc et al., 2006). The phylogenetic position of tunicates explains the growing interest towards these animals by researchers interested in various aspects of vertebrate evolution. Ascidians include Phlebobranchia, Stolidobranchia and Aplousobranchia, distinguished on the basis of pharynx morphology. They have an open circulatory system, and their haemolymph contains a great variety of circulating haemocytes with various roles. Ascidian haemocytes are the subject of a great deal of work reported in the scientific literature, as they are assumed to be involved in a variety of fundamental biological processes, including asexual reproduction and regeneration, tunic synthesis, detoxification and antioxidant responses, nutrient transportation, immune defence and allorecognition (Goodbody, 1974; Wright, 1981; Burighel and Cloney, 1997; Franchi et al., 2011, 2012, 2014, 2017; Ferro et al.

2013; Franchi and Ballarin, 2014, 2017). Most of the ultrastructural and cytochemical studies aimed at morpho-functional characterisation of ascidian haemocytes have been carried out in a limited number of species of Phlebobranchia (genus *Ascidia*, *Ciona*, *Perophora* and *Phallusia*) and Stolidobranchia (genus *Botryllus*, *Botrylloides*, *Styela*, *Polyandrocarpa* and *Halocynthia*), whereas no in-depth description of Aplousobranchia haemocytes is available in the literature. However, despite the abundant literature describing the morphology of living and fixed haemocytes (Pérès, 1943; Endean, 1955; Sabbadin, 1955; Andrew, 1961; Smith, 1970a,b; Schlumpberger et al., 1984; Sawada et al., 1991, 1993; Dan-Sohkawa et al., 1995) and their ultrastructure (Overton, 1966; Milanesi and Burighel, 1978; Scippa et al., 1982; Burighel et al., 1983; Zhang et al., 1992; Azumi et al., 1993; Sawada et al., 1993; Sugino et al., 1993), relatively few studies have addressed the biological functions of circulating ascidian cells. According to the available data, these cells can be grouped into a few functional categories, i.e., undifferentiated cells or haemoblasts, storage cells and immunocytes (Ballarin and Cima, 2005; Cima et al., 2016).

In previous studies, we carried out morpho-functional characterisations of the haemocytes of colonial stolidobranch species, such as *Botryllus schlosseri, Botrylloides leachii* and *Polyandrocarpa misakiensis*, which allowed us to obtain a better definition of their cell types and the roles of these cells in immune responses (Cima et al., 2001; Ballarin and Cima, 2005, Ballarin and Kawamura, 2009). In an attempt to increase our knowledge of ascidian haemocytes and contribute to the elucidation of some steps in the evolution of circulating cells within chordates, we extended our investigation to the haemolymph of *Diplosoma listerianum*, a colonial aplousobranch ascidian common in shallow waters of temperate regions although recent molecular data demonstrated a complex scenario of its global distribution comprising natural and human-mediated dispersal and cryptic diversity (Pérez-Portela et al., 2013). This species, easy to collect and rear under laboratory conditions, forms gelatinous colonies growing on algae, seagrasses and solid substrates, in which the minute zooids (up to 2 mm in length) are scattered. In contrast to botryllid ascidians, *Diplosoma* lacks a tunic vasculature connecting all of the zooids of a colony (Kott, 2001; Hirose and Akahori, 2004) and exhibits a limited number of circulating cells. Using electron and light microscopy analysis and a series of cytochemical, immunocytochemical, cytoenzymatic and lectin-specific procedures as well as functional assays, we were able to obtain a detailed description of *D. listerianum* haemocytes and their behaviour, and develop hypotheses regarding their functional roles.

2. Materials and Methods

2.2. Animals

Colonies of *Diplosoma listerianum* (Milne Edwards, 1841) were collected from the Lagoon of Venice, Italy, near the Marine Biological Station of the Department of Biology of the University of Padova, in Chioggia. The colonies were then transferred to glass slides and were maintained in aerated aquaria (temperature 17°C, salinity 35‰) and fed with Liquifry Marine (Liquifry Co., Dorking, UK).

2.3. Haemocyte collection

Colonies previously rinsed in 0.38% Na-citrate in filtered seawater (FSW), pH 7.5, to prevent haemocyte aggregation were gently dried with blotting paper, and zooids were disaggregated and torn using a fine tungsten needle causing the haemolymph leakage. The latter was collected with a glass micropipette, centrifuged at 780 x *g* for 10 min, and the pellet was re-suspended in FSW at a final concentration of 5 x 10^6 cells/ml. Next, 60 µl of the haemocyte suspension were placed in the centre of a culture chamber, prepared as described elsewhere (Cima, 2010), and left to adhere to a coverslip for 30 min at room temperature. Haemocytes were then treated as described below and finally observed under an Olympus CX31 light microscope (LM) equipped with a Lumenera 2 Infinity digital camera and Infinity Capture application v. 5.0.0 software (Lumenera Co., 2002-2009, Ottawa, ON) as well as an Amplified Fluorescence by Transmitted Excitation of Radiation (AFTER) LED fluorescence module (Fraen Corp., Corsico (Milan), Italy), with excitation at 365 nm (UV), 470 nm (FITC), and 535 nm (Cy3).

2.4. Cytochemical staining

All chemicals used in the experiments were obtained from Sigma-Aldrich Europe, except for those differently indicated.
Haemocytes were fixed for 30 min at 4°C using 4% paraformaldehyde plus 0.1% glutaraldehyde in 0.4 M cacodylate buffer containing 0.29 M NaCl and 29 mM sucrose.

The cells were then treated according to the following procedures, then washed in distilled water and mounted in Acquovitrex (Carlo Erba, Milan, Italy), an aqueous mounting solution, for observations under the LM.

Giemsa dye. Haemocytes were stained for 10 min in a 10% Giemsa solution and then washed in distilled water. Nuclei appeared blue and the cytoplasm appeared light blue or violet, due to metachromasia.

Toluidine blue. Fixed haemocytes were incubated for 5 s in 1% toluidine blue and 1% borax solution, pH 7.4, and then washed in distilled water. Basophilic components were stained blue.

Eosin. Fixed haemocytes were incubated for 10 s in 1% eosin Y in 80% ethanol and then washed in distilled water. Acidophilic sites were stained red.

Ehrlich's triacid mixture. Haemocytes were incubated in the Ehrlich's triacid mixture (12 vol saturated Orange G aqueous solution, 8 vol saturated acid fuchsin aqueous solution, 10 vol saturated methyl green aqueous solution, 30 vol distilled water, 18 vol absolute ethanol and 5 vol glycerine) for 15 min and then washed in distilled water (Bancroft and Gamble, 2002). Basophilic granules were light green; neutrophilic granules were violet; and acidophilic granules were copper red.

Periodic acid Schiff (PAS) reaction for polysaccharides. Fixed haemocytes were incubated in 1% periodic acid for 10 min, then rinsed in tap water and stained with Schiff's reagent for 30 min at 37°C. The coverslips were subsequently dipped in a solution of 0.6% sodium metabisulphite in 0.02 M HCl for 6 min, washed in tap water for 10 min, and rinsed in distilled water (Bancroft and Gamble, 2002). Positive sites appeared pinkish red.

Csaba staining for heparin. Haemocytes were incubated for 15 min in a solution of 0.36% Alcian Blue, 0.18% Safranin O, and 0.48% ammonium ferric sulphate in 0.1 M sodium acetate, pH 1.42 (Bancroft and Gamble, 2002). Non-sulphated heparin precursor appeared light blue, highly N-sulphated heparin appeared red.

Assay for polyphenols/quinones. Haemocytes were incubated for 30 min in a 2 mM solution of 3-methyl-2-benzothiazolinonehydrazone hydrochloride (MBTH) in FSW containing 0.4% N,N'-dimethylformamide (Franchi et al., 2015). Positive sites appeared red.

Masson-Fontana staining for polyphenols. After fixation, the haemocytes were incubated for 15 h in a solution of ammoniacal silver nitrate obtained by adding concentrated ammonia dropwise to 20 vol of 10% silver nitrate until the black precipitate disappeared and the solution became opalescent. Then, 20 vol of water was added, and the

haemocytes were incubated in this solution in the dark for 15 h (Bancroft and Gamble, 2002). The haemocytes were then washed in distilled water and incubated in a solution of 5% sodium thiosulphate and mounted.

2.5. Cytoenzymology

The following assays were carried out according to the methods reported in detail by Cima (2017). After incubation, haemocytes were washed in the appropriate buffer for 10 min and mounted in Acquovitrex.

β-Glucuronidase. After fixation, haemocytes were incubated in a reaction mixture containing naphthol AS-BI β-glucuronide as a substrate and hexazotised p-rosaniline as a chromogen in Na-acetate buffer, pH 5.2. Positive sites were stained red.

Alkaline phosphatase. After fixation, haemocytes were incubated for 2 h at 37°C in a reaction mixture containing naphthol AS-BI phosphate and hexazotised p-rosaniline as a chromogen in Tris–HCl buffer, pH 9.0. Positive sites appeared red.

Phenoloxidase. Fixed haemocytes were incubated for 60 min in a saturated solution of L-DOPA in phosphate-buffered saline (PBS: 1.37 M NaCl, 0.03 M KCl, 0.015 M KH_2PO_4, 0.065 M Na_2HPO_4, pH 7.2). Positive sites appeared dark brown.

2.6. Lectin cytochemistry

Biotin-conjugated concanavalin A (ConA, recognising α-D-glucopyranosides and α-D-mannopyranosides) and *Narcissus pseudonarcissus* agglutinin (NPA, specific for α-D-mannosyl carbohydrate residues) were assayed in haemocyte monolayers. Lectins were purchased from Sigma-Aldrich (ConA) and Vector, Burlingame, CA (NPA). After fixation, the haemocytes were incubated for 30 min in PBS containing 5% powdered milk, washed in PBS and incubated for 60 min in a 50 μg/ml lectin solution in PBS containing 0.1 mM $CaCl_2$. After the incubation, the haemocytes were washed in PBS, incubated for 30 min in avidin-biotin-peroxidase complex (Vector) in PBS, washed in PBS for 30 min, incubated for 5 min in 0.5 mg/ml of 3–3′ diaminobenzidine tetrahydrochloride (DAB) in PBS containing 0.04% H_2O_2, mounted in Acquovitrex and finally observed under the LM.

2.7. Immunocytochemical assays for heparin and histamine

Fixed haemocytes were incubated in a solution of 1% Evans Blue for autofluorescence quenching. The cells were then permeabilised for 5 min with 0.1% Triton X-100 in PBS, incubated in 10% normal goat serum (Vector) in PBS for 30 min to block aspecific reactions, and subsequently incubated with an anti-heparin mouse monoclonal antibody (MAB570 clone A7.10, Chemicon International, Temecula, CA) and an anti-histamine rabbit polyclonal antibody from synthetic histamine conjugated to succinylated KLH as immunogen (H7403, Sigma-Aldrich) at 10 µg/ml in PBS for 15 h at 4°C. In the controls, the primary antibodies were omitted. The haemocytes were then treated with biotin-conjugated goat anti-mouse Ig (401216, Calbiochem, San Diego, CA) for 60 min, followed by 30 min of incubation with streptavidin Cy3 (Sigma-Aldrich) at a concentration of 20 µg/ml in PBS for heparin detection. The same haemocytes were incubated in 10 µg/ml FITC-conjugated goat anti-rabbit IgG (401314, Calbiochem) for 60 min for histamine detection. Nuclear counterstaining was finally performed with 1 mg/ml diamidino-2-phenylindole (DAPI) for 30 min. The cells were finally washed in distilled water, mounted in FluorSave Reagent (Calbiochem), and observed under a fluorescence microscope. Negative controls were carried out by either omitting the primary antibody or by using primary antibodies pre-absorbed with antigen excess represented by of heparin sodium salt from porcine intestinal mucosa (Sigma, H7005) and histamine base (Fluka, 53290), respectively, at 100 µM concentration in PBS.

2.8. Degranulation assays

After adhesion on coverslip, haemocytes were incubated with 0.2 mM compound 48/80 in FSW for 15 min at 37°C and observed under the LM. In mammals, compound 48/80 triggers the degranulation of connective mast cells (Åbrink et al., 2004) via stimulation of trimeric G-proteins (Chahdi et al., 2000).
In another series of experiments, whole colonies were exposed to *Bacillus clausii* spores in FSW (4 x 10^8 spores/ml; Enterogermina, Sanofi, Milan, Italy) for 15 min at room temperature. They were then fixed for electron microscopy as described below.

2.9. Phagocytosis assay

A 60-µl aliquot of a haemocyte suspension was placed in the centre of a culture chamber, prepared as described by Cima (2010), and left to adhere to a coverslip for 30 min at room

temperature. After adhesion, haemocytes were incubated with 60 ml of a suspension of yeast cells (yeast:haemocyte ratio = 10:1) in FSW. They were then fixed, stained with Giemsa dye and observed under the LM. The percentage of cells with ingested yeast was estimated by counting the haemocytes (at least 200 cells for each monolayer) in 10 optic fields at a magnification of 1000x (0.21 mm viewfield diameter).

2.10. Electron microscopy

Selected pieces of *D. listerianum* colonies were fixed in a solution of 1.5% glutaraldehyde in 0.2 M cacodylate buffer, pH 7.4, plus 1.6% NaCl for 2 h at 4°C. They were then rinsed in cacodylate buffer containing 1.6% NaCl, post-fixed in 1.5% osmium tetroxide in cacodylate buffer, dehydrated and embedded in Epon. Thick sections (1 mm) were stained with toluidine blue. Ultrathin sections were briefly stained with uranyl acetate and lead citrate and then examined under an FEI TECNAI transmission electron microscope (TEM) equipped with a TIETZ high-resolution digital camera at 75 kV. Haemocytes were detected inside the entire zooids by observing the lacunae and sinuses of both the branchial basket and the mantle.

3. Results

3.1. The colony of D. listerianum

D. listerianum is a shallow-water species (occurring from the tidal zone to approximately 40 m in depth) that forms thin, flat encrusting colonies. The short zooids, constricted into thorax and abdomen by a narrow oesophageal neck, are scattered within the common translucent soft gelatinous tunic, where a muscular retractor process extends posteriorly obliquely outward from the thorax; the tunic lacks both a tunic vasculature and, in contrast to other didemnid genera, calcareous spicules. In each zooid, the oral siphon exhibits a separate opening to the exterior, whereas the exhalant aperture releases exhaust water in a wide atrial chamber connected with the exterior through a few large common cloacal openings (Fig. 1). Each colony is a clone, as it originates from the metamorphosis of a single tadpole-like larva into the founder oozooid and grows through a complex pyloric budding involving the epidermis and epicardium from the oesophageal region of the body.

3.2. The haemocytes of D. listerianum

Similar to all of the ascidians studied thus far, many haemocyte types are present in *D. listerianum*. On the basis of our analysis, we propose the following classification.

3.2.1. Haemoblast

This cell type is small in size (4-6 μm in diameter) and is usually found in clusters inside the haemolymph lacunae near the intestinal loops and the branchial basket, where mitotic figures can sometimes be observed. Under the LM, the haemoblast exhibits the typical features of an undifferentiated element (Fig. 2A). The cytoplasm appears homogeneous, uniformly stained, intensely basophilic with toluidine blue (Fig. 2B) and Giemsa dye (Fig. 2C) and is PAS positive (Fig. 2D). No granulations or other cytoplasmic specialisations can be observed. The nucleus occupies a large part of the cell volume and shows a centrally located, large, roundish nucleolus. Giemsa dye does not reveal chromatin clumps in the nucleus (Fig. 2C), which exhibits high alkaline phosphatase activity (Table 1).

Under the TEM, a high nucleocytoplasmic ratio is particularly evident (Fig. 2E). Most of the chromatin is dispersed, and the prominent nucleolus presents a granular texture. The cytoplasm contains some rounded or elongated mitochondria and a well-developed Golgi apparatus, near which a pair of centrioles can be observed. It also contains a large number of free ribosomes and polysomes and a few rough endoplasmic reticulum (RER) profiles, usually near the nucleus.

3.2.2. Hyaline amoebocyte

Under the LM, this cell type shows a variable shape, with a major axis of approximately 7-8 μm and a lower nucleocytoplasmic ratio than the haemoblast, without a visible nucleolus (Fig. 3A). It exhibits a roundish or ovoidal, well-developed nucleus, located centrally, without any particular features that can be observed with the nuclear dyes applied in this study (Fig. 3B). The cytoplasm appears homogeneous, clear and slightly basophilic (staining weakly light blue with Giemsa dye), revealing the presence of clear vesicles and fine acidophilic granulations (Fig. 3B) that are intensely positive for the PAS reaction (Fig. 3C) and the assays for alkaline phosphatase (Fig. 3D) and β-glucuronidase (Fig. 3E). This cell type forms long pseudopodia and is involved in phagocytosis, as confirmed *in vitro* after incubation of haemocytes with yeast cells (Fig. 3F).

TEM analysis shows the presence of a large number of cytoplasmic protrusions and the absence of clumps of chromatin or a nucleolus in the nucleus (Figs 3G,H). The cytoplasm

is filled with electron-dense particles with the characteristics of glycogen granules. It also contains many small vesicles, with an empty central region and a variable number of membrane-delimited granules filled with highly electron-dense contents (inset in Fig. 3H). The RER is underdeveloped, with scant cisternae and is generally located near the nucleus. The Golgi apparatus appears reduced and is formed by aligned short cisternae, from which vesicles containing electron-dense material similar to that found in the granules originate. Next to the Golgi apparatus, a pair of centrioles can often be observed. Mitochondria are numerous, roundish in shape and exhibit few cristae. Scarce droplets with lipid characteristics, which are not associated with membranes, are also present (Fig. 3G).

3.2.3. Macrophage-like cell

This cell type is highly variable in both size and shape, depending on its functional state (Fig. 4A). It is generally larger than 18 µm in size, and the nucleus is displaced to the periphery. It is found mainly in the haemolymph lacunae near the post-branchial digestive tract. Histochemical staining reveals a slightly basophilic cytoplasm, frequently containing granules and inclusions and sometimes including large heterophagic vacuoles (Fig. 4B). The contents of granules and vacuoles exhibit the same histochemical and histoenzymatic affinities as the hyaline amoebocyte (Figs 4C,D, Table 1), with which this cell type also shares the ability to phagocytise yeast cells *in vitro* (Fig. 4E).

At the ultrastructural level, the nucleus is easily visible in some sections; it lacks a nucleolus and appears roundish or flattened peripherally, near the plasmalemma. Chromatin forms electron-dense clumps lining the nuclear envelope. The cytoplasm contains few mitochondria, RER profiles, and lipid droplets. Similar to hyaline amoebocytes, both membrane-bound granules, with homogeneous electron-dense contents, and empty vesicles are also present. Most of the cell volume is occupied by large vacuoles (one or more) containing phagocytised material, including whole cells in some cases, at various stage of digestion (Fig. 4F).

3.2.4. Granular amoebocyte

This cell type is recognisable under the LM due to the presence of cytoplasmic granules that develop specific metachromatic staining with Giemsa dye (Fig. 5A), standing out from the basophilic cytoplasm (Fig. 5B) and showing positivity for the PAS reaction (Fig. 5C) and the phenoloxidase activity assay (Fig. 5D). This cell type exhibits a central roundish

nucleus that appears highly basophilic (Fig. 5B).

Under TEM analysis, this cell type, measuring approximately 7-8 μm and showing a variable form with many cytoplasmic protrusions, exhibits many clear vesicles and two types of membrane-bound granules (Figs 5E,F): the first type contains homogeneous material of low electron density, (Fig. 5G), and the second is large, strongly electron-dense and osmiophilic, with contents of various morphologies, from floccular (Fig. 5H) to homogeneous (Fig. 5F).

3.2.5. Morula cell

This cell type, which is roundish and up to 18 μm in diameter, is very frequent and exhibits many granules (Fig. 6A) that emit intense auto-fluorescence under UV light (Fig. 6B). Using Giemsa dye (Fig. 6C), Ehrlich's triacid mixture or eosin (Fig. 6D), the granules stain red, indicating their highly acidophilic nature. They are also PAS positive (Fig. 6E), contain polyphenolic substances (Figs 6F,G), and are positive for the activities of enzymes (Table 1) such as alkaline phosphatase (Fig. 6H) and phenoloxidase (Fig. 6I). Following bacterial stimulation, these cells degranulate (Fig. 7A); the granules appear smaller and are displaced at the periphery of the cell, and oxidation of their polyphenolic content is evident (Fig. 7B).

The cytoplasm ultrastructure (Fig. 6J) appears very similar to that of the granular amoebocyte, but unlike that cell type, clear vesicles and granules with homogeneous contents of low electron density are scarce, whereas large and strongly electron-dense granules prevail, filling almost the entire cytoplasm and exhibiting a more uniform content with few less electron-dense areas (Fig. 6K). Numerous RER profiles are present. The nucleus may have a nucleolus. When these cells degranulate as a result of immune stimuli, large granules are displaced at the cell periphery, with some undergoing coalescence (Fig. 7C), and they appear to lose their electron-dense contents to various degrees (Figs 7D,E), part of which remains along the interior side of the granule membrane (Fig. 7F).

3.2.6. Mast cell-like granulocyte

This cell type has a size of 6-8 μm and exhibits a peripheral nucleus (Fig. 8A). The cytoplasm stains weakly with Giemsa dye, whereas granules are strongly basophilic (Fig. 8B) and PAS positive (Fig. 8C). Using Ehrlich's triacid mixture, the granules stain dark green, confirming their high basophilia (Fig. 8D). With Csaba's mixture (Fig. 8E), the

granules are predominantly blue, supporting the presence of weakly or non-sulphated glucosaminoglycans, with pink veins, indicating the probable presence of highly sulphated heparin (Table 1). Immunocytochemical assays show that histamine is located within the granules (Fig. 8F), whereas heparin is displaced peripherally along the interior side of the granule membrane (Fig. 8G). This is the only cell type able to respond to the presence of the compound 48/80 with degranulation, and only few granules remain at the cell periphery following incubation with this compound (Fig. 8H). Finally, the surface of this cell type binds ConA (Fig. 8I) and NPA with high affinity (Table 1).

Rare short cytoplasmic protrusions are observable under the TEM. The eccentric nucleus shows chromatin clumping, and the scarce cytoplasm is filled with membrane-delimited granules (Fig. 8J). The content of the granules is of low electron density and exhibits a granular or filamentous appearance, except in a small central, highly electron-dense core (Fig. 8K). Among the granules, some mitochondria and scarce RER profiles can be detected.

3.2.7. Spherule cell

This cell type is variable in size, ranging between 7 and 18 µm. LM analysis reveals a vacuolated cell with little basophilic cytoplasm. Vacuoles appear filled with fine granular material (Fig. 9A) and are PAS positive (Fig. 9B).

The TEM provides more detailed information (Figs 9C,E). The nucleus exhibits a peripheral position and shows a large nucleolus. In the cytoplasm, scarce mitochondria and some RER profiles are present along the periphery. The salient feature of this cell type is the presence of a Golgi apparatus, which is enormously developed and displaced in the central area of the cell (Figs 9E,F); its cisternae extend peripherally into large sheets that collectively form a honeycomb structure when viewed in sections, due to regular expansions of the cisternae, separated by narrow cisternal tracts. At the periphery, these expansions form roundish vesicular structures that increase in both number and volume, becoming large vacuoles containing homogeneous material of low electron density, with a more electron-dense filamentous central portion (Fig. 9D).

3.2.8. Nephrocyte

This cell type is variable in shape and is characterised by the presence of numerous birefringent granules, which are clearly visible when observed under the LM with a 45°-incident light (Fig. 10A).

The most evident feature of its ultrastructure is the presence of vacuoles containing material arranged in crystalline filaments (Fig. 10B) that assume a regular structure, forming parallel chains (Fig. 10C) or hexagonal motifs (Fig. 10D) depending on the type of section. The nucleus may present a small peripheral nucleolus. Scarce roundish or ovoidal mitochondria and RER profiles are present in the cytoplasm, together with a well-developed Golgi apparatus (Fig. 10B).

4. Discussion

Despite the numerous studies on ascidian haemocytes, there is a general lack of information about circulating cells of Aplousobranchia, including their morphology and possible functions. General histological and supravital stains were employed in the first half of the 20th century as an attempt for classifying the haemocytes of some species of aplousobranch ascidians by some authors, such as Azéma, George and Pérès (reported in Wright, 1981) causing the development of a variety of generic morphological terms, which had scarce scientific consent in the following years and were abandoned because appeared difficult to compare. In the present work, we studied the morphological, cytochemical and cytoenzymatic features of the haemocytes of *D. listerianum*, a common aplousobranch ascidian, using staining methods for light microscopy; for a better morpho-functional characterisation, we analysed their ultrastructure in detail and acquired information about their behaviour when challenged with non-self microbes, such as yeast cells and *B. clausii* spores. Results were finally compared with those reported in other ascidians to share a common terminology which can be useful in cell type classification (Table 2).

We identified eight different morphotypes: haemoblasts, hyaline amoebocytes, macrophage-like cells, granular amoebocytes, morula cells, mast cell-like granulocytes, spherule cells and nephrocytes.

Haemoblasts are mobile elements that are probably pluripotent and are considered the founder cells of ascidian haemolymph cells. Their ability to reproduce and differentiate into other circulating cell types has been reported by various authors (Ermak, 1976; Milanesi and Burighel, 1978; Wright and Ermak, 1982; Rowley et al., 1984; Sawada et al., 1993; Cima et al., 2001; Hirose et al., 2003; Amano and Hori, 2008; Voskoboynik et al., 2008; Rinkevich et al., 2013). Our observations are consistent with this hypothesis, as these cells morphologically correspond to the undifferentiated elements proposed by the above

authors. We observed circulating haemoblasts with mitotic figures; in addition, alkaline phosphatase activity was present in the nucleus, which is directly correlated with growth and cell proliferation (Chévremont and Firket, 1953). This enzyme activity disappears in the nucleus of committed not-proliferating cells. The large nucleolus and richness of polysomes are related to intense synthesis of RNA and proteins in haemoblasts. The prevalence of polysomes on the RER cisternae suggests that structural proteins are synthesised to meet the needs of rapid cell differentiation. In the absence of a cellular microenvironment, cell commitment is likely due to input from pathogens, cytokines, and interaction between humoral and cell immune reactions (Donaghy et al., 2017), although the histogenesis of the various lines of differentiation is still unknown. Transcriptome analysis and molecular techniques will allow to find useful markers to label circulating haemoblasts and follow their differentiation/maturation fate.

Hyaline amoebocytes are phagocytes with remarkable motility. Under the TEM, various phases of cell differentiation were observed. This cell type might derive from haemoblasts after the acquisition of cytoplasmic vesicles. In young cells, the nucleocytoplasmic ratio is still high, and compared with haemoblasts, free ribosomes decrease in number, and the cytoplasm becomes less basophilic. As differentiation proceeds, the nucleocytoplasmic ratio decreases, chromatin clumps, the Golgi apparatus develops, vesicles increase in number, and those with electron-dense content converge to form membrane-bound granules, which are abundant in differentiated amoebocytes and likely represent lysosomes. The ultrastructure of this cell type has been described in various ascidian species. In the phlebobranch *Ciona intestinalis*, it corresponds to non-vacuolar hyaline amoebocytes (Rowley, 1982) and clear vesicular granulocytes (Scippa and Izzo, 1996). In stolidobranch Styelidae, it corresponds to the hyaline cells of *Styela clava* (Sawada et al., 1993) and the hyaline amoebocytes of botryllids (Cima et al., 2001); the latter cell type was formerly known as microgranular amoebocytes (Milanesi and Burighel, 1978).

Macrophage-like cells exhibit cytochemical and ultrastructural features that are comparable with those of hyaline amoebocytes, from which they probably derive representing a terminal differentiation of the phagocytic line, as previously demonstrated in the stolidobranch colonial ascidian *Botryllus schlosseri* (Ballarin and Cima, 2005). Ultrastructural analysis showed that the shape of the nucleus and the chromatin distribution as well as the type of granules and vesicles observed in the cytoplasm share high similarity with hyaline amoebocytes. This cell type is able to phagocytise target particles (yeast cells) *in vitro*. In ascidians, phagocytosis is required not only for immune

responses against potentially pathogenic microorganisms but also for the clearance of damaged/effete cells and apoptotic bodies during the metamorphosis of the larva and zooid resorption. The last process occurs both cyclically, during the recurrent alternation of generations of botryllid ascidians, and in the case of hibernation and aestivation, to overcome adverse weather conditions. In all of these cases, a significant increase in the number of macrophage-like cells is observed in the haemolymph, likely due to their rapid differentiation from the hyaline amoebocytes (Burighel et al., 1976; Cloney, 1982; Cima et al., 2003; Ballarin et al., 2008; Cima et al., 2010). This cell type shares ultrastructural features with the phagocytes of stolidobranchs, such as botryllids (Hirose et al., 2003), *Polyandrocarpa* (Ballarin and Kawamura, 2009) and pyurids (Zhang et al., 1992), as well as the vacuolar hyaline amoebocytes of phlebobranchs, such as *Ciona intestinalis* (Rowley, 1982), *Phallusia mammillata* (Scippa and Iazzetti, 1989), and *Phallusia nigra* (de Barros et al., 2014). Collectively, the above data support our previous proposal of hyaline amoebocytes and macrophage-like cells as two developmental steps of the same immunocyte type with phagocytic ability (Cima et al., 2001; Ballarin and Cima, 2005; Cima et al., 2016).

Granular amoebocytes and morula cells both exhibit the presence of acidophilic granules with strong osmiophily in their cytoplasm, strengthening our previous hypothesis that they represent two differentiation steps of a single cell type (Ballarin and Cima, 2005). In botryllid ascidians, granular amoebocytes were formerly known as macrogranular amoebocytes (Milanesi and Burighel, 1978). In stolidobranch botryllids and styelids, morula cells are round and contain several vacuoles, in various sizes and numbers, which are filled with electron-dense material (Milanesi and Burighel, 1978; Sawada et al., 1993; Cima et al., 2001; Hirose et al., 2003; de Barros et al., 2009; Ballarin and Kawamura, 2009). These characteristics have also been recognised in the same cell type of phlebobranch Ascidiidae, such as *P. mammillata* (Scippa and Iazzetti, 1989) and *P. nigra* (de Barros et al., 2014), as well as Cionidae (Di Bella et al., 2011). In Stolidobranchia, morula cells accumulate iron and were previously referred to as ferrocytes by various authors to distinguish them from vanadocytes, containing vanabins or haemovanadin (a group of vanadium-binding metalloproteins) in Aplousobranchia and Phlebobranchia, which generally accumulate high levels of vanadium (Michibata, 1989; Kustin et al., 1990). However, vanadocytes are not morula cells. They are univacuolated cells, which are also known as signet-ring cells due to the presence of a single large vacuole, with homogeneous, strongly electron-dense contents that occupy most of the cell and force the

discoid nucleus to one side (Yamaguchi et al., 2006; Ballarin, 2012; de Barros et al., 2014). In the case of *D. listerianum*, cells with the morphology of vanadocytes (i.e., large signet-ring cells) were not found, and the presence of this cell type in this species is therefore still uncertain.

Analogous to other ascidians (Ballarin, 2012; Franchi et al., 2015), *Diplosoma* morula cells contain polyphenolic compounds inside their granules, likely represented by tunichromes, which are considered to be fragments of DOPA-containing proteins and the substrate of phenoloxidase (Sugumaran and Robinson, 2012; Franchi et al., 2015), the oxidative enzyme which is also present in *Diplosoma* morula cells. Morula cells, tunichromes and phenoloxidase are involved in various ascidian biological processes, such as tunic formation/regeneration and inflammatory responses leading to cytotoxicity and melanisation, which are particularly evident in allorejection reaction of compound ascidians (Sugumaran and Robinson, 2012; Franchi et al., 2015; Franchi and Ballarin, 2016).

The mast cell-like granulocytes derive their name from their histochemical properties, i.e., the presence of histamine and heparin inside the granules and the ability to respond quickly to the compound 48/80, which induces degranulation of mammalian mast cells (Åbrink et al., 2004). The mast cell-like granulocytes of *D. listerianum* share features such as an eccentric nucleus and the presence of many small granules with an electron-dense core and a clear outer shell with the basophilic granulocytes of stolidobranch styelids (Sawada et al., 1993; Cima et al., 2001; Hirose et al., 2003; de Barros et al., 2009) and pyurids (Zhang et al., 1992; Fuke and Fukumoto, 1993). In *S. plicata*, immunohistochemical and TEM analyses showed co-localisation of heparin and histamine inside the granules of granulocytes, which might act as basophil-like granulocytes in innate immune responses (de Barros et al., 2007). In this species, histamine is secreted after a pathogenic stimulus, which decreases phagocytic ability and promotes vasoconstriction in tunic explants, supporting the hypothesis of its involvement in the regulation of inflammation and host defence (García-García et al., 2014). In *B. leachii*, granular cells have been observed to cross the basal membrane and infiltrate the gut epithelium. A role in immunosurveillance of the alimentary tract, similar to that exerted by mammalian mucosal mast cells, has been hypothesised, which is supported by positivity to β-glucuronidase and chloroacetylesterase, two enzymes found inside the granules of mammalian mast cells that are involved in the digestion of mucosal connective tissue (Cima et al., 2001). The observed affinity of *Diplosoma* mast cell-like granulocytes for ConA and NPA indicates the presence of surface carbohydrates that might be related to

mast cell-like functions, as mannose/glucose-binding lectins stimulate histamine release in mammalian peritoneal mast cells (Gomes et al., 1994).

Spherule cells are haemocytes with characteristics that have never been observed previously in other ascidian species. These cells exhibit a Golgi apparatus that develops to a large extent and numerous vacuoles with fine granular contents. Their role is not easy to interpret. The extensive development of the Golgi apparatus and the numerous vesicles that form at the sides of the long cisternae suggests high accumulation of material to be used according to the particular needs of the zooid. In particular, the ultrastructure and the staining properties of the vacuolar content are similar to those of the spherulocytes found in the haemolymph of insects and echinoderms (Smith, 1981). It has been hypothesised that these spherulocytes exhibit mucopolysaccharidic contents that are secreted into the extracellular space during regeneration events (García-Arrarás et al., 2006) and are involved in the formation and maintenance of the extracellular matrix, like vertebrate fibroblasts (Byrne, 1986). Therefore, the possibility that this cell type might be involved in tunic fibrogenesis favouring the deposition and modification of tunicin fibrils and/or collagenous fibres in *D. listerianum* cannot be excluded. In regard to other ascidians, globular granulocytes (Scippa and Izzo, 1996) and fibrous-material containing cells (Zhang et al., 1992), also known as giant cells (Fuke and Fukumoto, 1993; Amano and Hori, 2008) were previously reported in the phlebobranch *Ciona intestinalis* and the pyurid stolidobranch *Halocynthia roretzi*, respectively. A role in tunic formation has been proposed for the glomerulocytes of the styelid *Polyandrocarpa misakiensis*, which contains intracytoplasmic fibrous material resembling tunic fibres (Mukai et al., 1990). These fibres, consisting of cellulose I (Kimura and Itoh, 1995), are not only involved in tunic formation but can also form a network in the haemocoel as a primary scaffold for other components of the extracellular matrix (Kimura and Itoh, 1997). Since cellulose synthases are transmembrane proteins found in ascidian epidermis (Matthysse et al., 2004) and Hirose and Mukai (1992) demonstrated that these large circulating cells are derived from epidermal cells, their role appear an intriguing question.

Unlike the nephrocytes of Stolidobranchia, in *D. listerianum*, this cell type is variable in shape and does not contain large vacuoles. Within its vacuoles, the filaments gradually organise themselves into paracrystalline structures. These cells accumulate nitrogenous catabolites with typical birefringence inside their vacuoles, as observed in other ascidians; for example, the nephrocytes of the stolidobranch colonial ascidian *B. schlosseri* accumulate uric acid (Sabbadin and Tontodonati, 1967; Ballarin and Cima, 2005) and

exhibit hourglass-shaped crystals inside large vacuoles (Milanesi and Burighel, 1978). In phlebobranch ascidians and thaliaceans, nephrocyte vacuoles contain a network of tophi-like tubular crystals (Cima et al., 2014). The particular hexagonal shape of the crystals in conglomerates observed in *D. listerianum* might be related to the precipitation of crystals of urate or cystine (Fogazzi, 1996).

5. Conclusion

This study characterised the haemocytes of *D. listerianum* for the first time. These cells show commonalities (many) and differences (few) compared with the haemocytes of other ascidians previously described. Although aplousobranchs are phylogenetically related to phlebobranch ascidians, *D. listerianum* lacks both the refractile amoebocytes and univacuolated cells (or signet-ring cells, or vanadocytes) that are commonly found in phlebobranchs. Further investigations extended to other aplousobranch species will be required to confirm these differences. This study also aims to add another contribution to the shared classification of ascidian haemocytes, which is fundamental for supporting the emerging molecular data. Morphology and genetics are now providing new and unexpected clues for understanding the roles of ascidian circulating cells in biological processes such as blastogenesis and differentiation (Laird et al., 2005; Rinkevich et al., 2007, 2013; Gasparini et al., 2015) as well as stress/immune responses (Franchi and Ballarin, 2014, 2017; Franchi et al., 2011a,b, 2012, 2013, 2014, 2017; Ferro et al., 2013; Vizzini et al., 2013, 2015, 2016). The increasing availability of various transcriptomes in the near future will certainly contribute to the clarification of some obscure aspects of ascidian haemocytes.

Conflict of interest

The authors declare no conflict of interest. “None”.

Acknowledgements

The authors wish to thank Dr. Federico Caicci for electron microscopy support and TEM images. This work was supported by the Italian MIUR (Ministry of Education, University and Research). The English text was revised by American Journal Experts (AJE, http://www.journalexperts.com/, certificate #90F3-8ECA-3EA7-8FCD-AEF3).

References

Åbrink, M,, Grujic, M., Pejler, G., 2004. Serglycin is essential for maturation of mast cell secretory granule. J. Biol. Chem. 279, 40897-40905.

Amano, S., Hori, I., 2008. Hemocyte differentiation in the juveniles of the ascidian *Halocynthia roretzi*. Invertebr. Repr. Dev. 51, 11-18.

Andrew, W. 1961. Phase microscope studies of living blood-cells of the tunicates under normal and experimental conditions, with a description of a new type of motile cell appendage. Quart. J. Microscop. Sci. 102, 89-105.

Azumi, K., Satoh, N., Yokosawa, H., 1993. Functional and structural characterization of hemocytes of the solitary ascidian, *Halocynthia roretzi*. J. Exp. Zool. 265, 309-316.

Ballarin, L., 2012. Ascidian cytotoxic cells: state of the art and research perspectives. ISJ-Invertebr. Surv. J. 9, 1-6.

Ballarin, L., Cima, F., 2005. Cytochemical properties of *Botryllus schlosseri* haemocytes: indications for morpho-functional characterisation. Eur. J. Histochem. 49, 255-264.

Ballarin, L., Kawamura, K., 2009. The hemocytes of *Polyandrocarpa misakiensis*: morphology and immune-related activities. ISJ-Invertebr. Surv. J., 154-161.

Ballarin, L., Menin, A., Tallandini, L., Matozzo, V., Burighel, P., Basso, G., Fortunato, E., Cima, F., 2008. Haemocytes and blastogenetic cycle in the colonial ascidian *Botryllus schlosseri*: a matter of life and death. Cell Tissue Res. 331, 555-564.

Bancroft, J.D., Gamble, M., 2002. Theory and Practice of Histological Techniques. Churchill Livingstone, London.

Burighel, P., Cloney, R.A., 1997. Urochordata: Ascidiacea, in: Harrison F.W., Ruppert E.E. (Eds.), Microscopic Anatomy of Invertebrates, vol. 15. Hemichordata, Chaetognatha, and the Invertebrate Chordates. Wiley-Liss Inc, New York, pp. 221-347.

Burighel, P., Brunetti, R., Zaniolo, G., 1976. Hibernation of the colonial ascidian *Botrylloides leachi* (Savigny): Histological observations. Boll. Zool. 43, 293-301.

Burighel, P., Milanesi, C., Sabbadin, A., 1983. Blood cell ultrastructure of the ascidian *Botryllus schlosseri*. II. Pigment cells. Acta Zool. 64,15-23.

Byrne, M., 1986. The ultrastructure of the morula cells of *Eupenctacta quinquesemita* (Echinodermata: Holothuroidea) and their role in the maintenance of the extracellular matrix. J. Morphol. 188,179-189.

Chahdi, A., Fraundorfer, P.F., Beaven, M.A., 2000. Compound 48/80 activates mast cells phospholipase D via heterotrimeric GTP-binding proteins. J. Pharmacol. Exp. Ther. 292, 122-130.

Chèvremont, M., Firket, H., 1953. Alkaline phosphatase of the nucleus. Int. Rev. Cytol. 2, 261-288.

Cima, F., 2010. Microscopy methods for morpho-functional characterisation of marine invertebrate haemocytes, in: Méndez-Vilas, A., Álvarez, J.D. (Eds.), Microscopy: Science, Technology, Applications and Education, Vol. 2, Microscopy Book Series – N. 4 Formatex Research Center, Badajoz, pp 1100-1107 http://www.formatex.org/microscopy4/index.html

Cima, F., 2017. Enzyme histochemistry for functional histology in invertebrates, in: Pellicciari, C., Biggiogera, M. (Eds.), Single Molecule Histochemistry: Methods and Protocols. Methods in Molecular Biology, vol. 1560, Springer Protocols, Humana Press, Springer Science, New York, pp. 69-90.

Cima, F., Perin, A., Burighel, P., Ballarin, L., 2001. Morpho-functional characterisation of haemocytes of the compound ascidian *Botrylloides leachi* (Tunicata, Ascidiacea). Acta Zool. 82, 261-274.

Cima, F., Basso, G., Ballarin, L., 2003. Apoptosis and phosphatidylserine-mediated recognition during the take-over of the colonial life-cycle in the ascidian *Botryllus schlosseri*. Cell Tissue Res. 312, 369-376.

Cima, F., Manni, L., Basso, G., Fortunato, E., Accordi, B., Schiavon, F., Ballarin, L., 2010. Hovering between death and life: natural apoptosis and phagocytes in the blastogenetic cycle of the colonial ascidian *Botryllus schlosseri*. Dev. Comp. Immunol. 34, 272-285.

Cima, F., Caicci, F., Sordino, P., 2014. The haemocytes of the salp *Thalia democratica* (Tunicata, Thaliacea): an ultrastructural and histochemical study in the oozoid. Acta Zool. 95, 375-391.

Cima, F., Franchi, N., Ballarin, L., 2016. Origin and function of tunicate hemocytes, in: Malagoli, D. (Ed.), The Evolution of the Immune System, chapter 2, Elsevier, London, pp. 29-49.

Cloney, R.A., 1982. Ascidian larvae and the events of metamorphosis. Am. Zool. 22, 817-826.

Dam, T.K., Brewer, C.F., 2002. Thermodynamic studies of lectin-carbohydrate interactions by isothermal titration calorimetry. Chem. Rev. 102, 387-429.

Dan-Sohkawa, M, Morimoto, M., Kaneko, H., 1995. *In vitro* reactions of coelomocytes against sheep red blood cells in the solitary ascidian *Halocynthia roretzi*. Zool. Sci. 12, 411- 417.

de Barros, C.M., Andrade, L.R., Allodi, S., Viskov, C., Mourier, P.A., Cavalcante, M.C.M., Straus, A.H., Takahashi, H.K., Pomin, V.H., Carvalho, V.F., Martins, M.A., Pavão, M.S.G., 2007. The hemolymph of the ascidian *Styela plicata* (Chordata-Tunicata) contains heparin inside basophil-like cells and a unique sulphated galactoglucan in the plasma. J. Biol. Chem. 282,1615-1626.

de Barros, C.M., De Carvalho, D.R., Andrade, L.R., Pavão, M.S.G., Allodi, S., 2009 Nitric oxide production by hemocytes of the ascidian *Styela plicata*. Cell Tissue Res. 339, 117-128.

de Barros, C.M., Emrich, L.C., Mello, A., Da Fonseca, R.N., Allodi, S., 2014. Regulation of nitric-oxide production in hemocytes of the ascidian *Phallusia nigra*. Nitric Oxide 38, 26-36.

Delsuc, F., Brinkmann ,H., Chourrout, D., Philippe, H., 2006. Tunicates and not cephalochordates are the closest living relatives of vertebrates. Nature 439, 965-968.

Di Bella, M.A., Fedders, H., De Leo, G., Leippe, M., 2011 Localization of antimicrobial peptides in the tunic of *Ciona intestinalis* (Ascidiacea, Tunicata) and their involvement in local inflammatory-like reactions. Results Immunol. 1, 70-75.

Donaghy, L., Hong, H-K., Park, K-I, Nobuhisa, K., Youn, S-H., Kang, C-K., Choi, K-S., 2017. Flow cytometric characterization of hemocytes of the solitary ascidian, *Halocynthia roretzi*. Fish Shellfish Immunol. 66, 289-299.

Endean, R., 1955. Studies of the blood and tests of some Australian ascidians. I. Blood of *Pyura stolonifera*. Aust. J. Mar. Freshwater Res. 6, 35-59.

Ermak, T.H., 1976. The hematogenic tissues of tunicates, in: Wright, R.H., Cooper, E.L. (Eds.), Phylogeny of Thymus and Bone Marrow-Bursa Cells, Elsevier, Amsterdam, pp. 45-56.

Ferro, D., Franchi, N., Ballarin, L., Cammarata, M., Mangano, V., Rigers, B., Parrinello, N., Santovito, G., 2013. Characterization and metal-induced gene transcription of two new copper zinc superoxide dismutases in the solitary ascidian *Ciona intestinalis*. Aquat. Toxicol. 140-141, 369-379.

Fogazzi, G.B., 1996. Crystalluria: a neglected aspect of urinary sediment analysis. Nephrol. Dial. Transplant. 11, 379-387.

Franchi, N., Ballarin, L., 2014. Preliminary characterization of complement in a colonial tunicate: C3, Bf and inhibition of C3 opsonic activity by compstatin. Dev. Comp. Immunol. 46, 430-438.

Franchi, N., Ballarin, L., 2016. Cytotoxic cells of compound ascidians, in: Ballarin, L., Cammarata, M. (Eds.) Lessons in Immunity: From Single-cell Organisms to Mammals, chapter 14, Elsevier, London, pp. 193-203.

Franchi, N., Ballarin, L., 2017. Morula cells as key hemocytes of the lectin pathway of complement activation in the colonial tunicate *Botryllus schlosseri*. Fish Shellfish Immunol. 63, 157-164.

Franchi, N., Boldrin, F., Ballarin, L., Piccinni, E., 2011. CiMT-1, an unusual chordate metallothionein gene in *Ciona intestinalis* genome: structure and expression studies. J. Exp. Zool. 315A, 90-100.

Franchi, N., Ferro, D., Ballarin, L., Santovito, G., 2012. Transcription of genes involved in glutathione biosynthesis in the solitary tunicate *Ciona intestinalis* exposed to metals. Aquat. Toxicol. 114-115, 14-22.

Franchi, N., Piccinni, E., Ferro, D., Basso, G., Spolaore, B., Santovito, G., Ballarin, L., 2014. Characterization and transcription studies of a phytochelatin synthase gene from the solitary tunicate *Ciona intestinalis* exposed to cadmium. Aquat. Toxicol. 152, 47-56.

Franchi, N., Ballarin, L., Cima, F., 2015. Insights on cytotoxic cells of the colonial ascidian *Botryllus schlosseri*. ISJ-Invertebr. Surv. J. 12, 109-117.

Franchi, N., Ballin, F., Ballarin, L., 2017. Protection from oxidative stress in immunocytes of the colonial ascidian *Botryllus schlosseri*: transcript characterization and expression studies. Biol. Bull. 232, 45-57.

Fuke, M., Fukumoto, M., 1993. Correlative fine structural, behavioral, and histochemical analysis of ascidian blood cells. Acta Zool. 74, 61–71.

García-Arrarás, J.E., Schenk, C., Rodrígues-Ramírez, R., Torres, I.I., Valentín, G., Candelaria, A.G., 2006. Spherulocytes in the echinoderm *Holothuria glaberrima* and their involvement in intestinal regeneration. Dev. Dyn. 235: 3259-3267.

García-García, E., Gómez-González, N.E., Meseguer, J., García-Ayala, A., Victoriano Mulero, V., 2014. Histamine regulates the inflammatory response of the tunicate *Styela plicata*. Dev. Comp. Immunol. 46, 382-391.

Gasparini, F., Manni, L., Cima, F., Zaniolo, G., Burighel, P., Caicci, F., Franchi, N., Schiavon, F., Rigon, F., Campagna, D., Ballarin, L., 2015. Sexual and asexual reproduction in the colonial ascidian *Botryllus schlosseri*. Genesis 53, 105-120.

Gomes, J.C., Rossi Ferreira, R., Sousa Cavada, B., Azevedo Moreira, R., Oliveira, J.T.A., 1994. Histamine release induced by glucose (mannose)-specific lectins isolated from Brazilian beans. Comparison with concanavalin A. Agents Actions 41, 132-135.

Goodbody, I., 1974. The physiology of ascidians. Adv. Mar. Biol. 12, 1-149.

Hirose, E., Akahori, M., 2004. Comparative morphology of the stolonic vessel in a didemnid ascidian and some related tissues in colonial ascidians. Zool. Sci. 21, 445-455.

Hirose, E., Mukai H., 1992. An ultrastructural study on the origin of glomerulocytes, a type of blood cell in a styelid ascidian *Polyandrocarpa misakiensis*. J. Morphol. 211, 269-273.

Hirose, E., Shirae, M., Saito, Y., 2003. Ultrastructure and classification of circulating hemocytes in 9 botryllid ascidians (Chordata: Ascidiacea). Zool. Sci. 20, 647-656.

Kimura, S., Itoh, T., 1995. Evidence for the role of glomerulocyte in cellulose synthesis in the tunicate *Metandrocarpa uedai*. Protoplasma 186, 24-33.

Kimura, S., Itoh, T., 1997. Cellulose network of hemocoel in selected compound styelid ascidians. J. Electron. Microsc. 46, 327-335.

Kott, P., 2001. The Australian Ascidiacea. Part 4, Aplousobranchia (3), Didemnidae. Mem. Queensl. Mus. 47, 1-407.

Kustin, K., Robinson, W.E., Smith, M.J., 1990. Tunichromes, vanadium, and vacuolated blood cells in tunicates. Invertebr. Repr. Dev. 17,129-139.

Laird, D.J., De Tomaso, A.W., Weissman, I.L., 2005. Stem cells are units of natural selection in a colonial ascidian. Cell 123, 1351-1360.

Matthysse, A.G., Deschet, K., Williams, M., Marry, M., White, A.R., Smith, W.C., 2004. A functional cellulose synthase from ascidian epidermis. Proc. Natl. Acad. Sci. USA 101, 986-991.

Michibata, H., 1989. New aspects of accumulation and reduction of vanadium ions in ascidians, based on concerted investigation for both a chemical and biological point of view. Zool. Sci. 6, 639-647.

Milanesi, C., Burighel, P., 1978. Blood cell ultrastructure of the ascidian *Botryllus schlosseri*. I. Hemoblast, granulocytes, macrophage, morula cell and nephrocyte. Acta Zool. 59, 135-147.

Mukai, H., Hashimoto, K., Watanabe, H., 1990. Tunic cords, glomerulocytes, and eosinophilic bodies in a styelid ascidian, *Polyandrocarpa misakiensis*. J. Morphol. 206, 197-210.

Overton, J., 1966. The fine structure of blood cells in the ascidian *Perophora viridis*. J. Morphol .119, 305-326.

Pérès, J.M., 1943. Recherches sur le sang et les organs neuraux des tuniciers. Ann. Inst. Oceanogr. 21,229-359.

Pérez-Portela, R., Arranz, V.,Rius, M., Turon, X., 2013. Cryptic speciation or global spread? The case of a cosmopolitan marine invertebrate with limited dispersal capabilities. Sci. Rep. 3, 3197.

Rinkevich, Y., Douek, J., Haber, O., Rinkevich, B., Reshef, R., 2007. Urochordate whole body regeneration inaugurates a diverse innate immune signaling profile. Dev. Biol. 312, 131-146.

Rinkevich, Y., Voskoboynik, A., Rosner, A., Rabinowitz, C., Paz, G., Oren, M., Douek, J., Alfassi, G., Moiseeva, E., Ishizuka, K.J., Palmeri, K.J., Weissman, I.L., Rinkevich, B., 2013. Repeated, long-term cycling of putative stem cells between niches in a basal chordate. Dev. Cell 24, 76-88.

Rowley, A.F., 1982. Ultrastructural and cytochemical studies on the blood cells of the sea squirt, *Ciona intestinalis*. I. Stem cells and amoebocytes. Cell Tissue Res. 223, 403-414.

Rowley, A.F., Rhodes, C.P., Ratcliffe, N.A., 1984. Protochordate leucocytes. A review. Zool. J. Linn. Soc. 80, 283-295.

Sabbadin, A. 1955. Studio sulle cellule del sangue di *Botryllus schlosseri* (Pallas) (Ascidiacea). Arch. Ital. Anat. Embriol. 60, 33-67.

Sabbadin, A., Tontodonati, A., 1967. Nitrogenous excretion in the compound ascidian *Botryllus schlosseri* (Pallas) and *Botrylloides leachi* (Savigny). Monit. Zool. It. 1, 185-190.

Sawada, T., Fujikura, Y., Tomonaga, S., Fukumoto, T., 1991 Classification and characterization of ten hemocyte types in the tunicate *Halocynthia roretzi*. Zool. Sci. 8, 939-950.

Sawada, T., Zhang, J., Cooper, E.L., 1993. Classification and characterization of hemocytes in *Styela clava*. Biol. Bull. 184, 87-96.

Schlumpberger, J.M., Weissman, I.L., Scofield, V.L., 1984. Separation and labeling of specific subpopulations of *Botryllus* blood cells. J. Exp. Zool. 229, 401-411.

Scippa, S., Botte, L., De Vincentiis, M., 1982. Ultrastructure and X-ray microanalysis of blood cells of *Ascidia malaca*. Acta Zool. 63, 121-131.

Scippa, S., Iazzetti, G., 1989. Studio ultrastrutturale sulle cellule del sangue dell'ascidiaceo *Phallusia mammillata*. Obelia 15, 935-938.

Scippa, S., Izzo, C., 1996. An ultrastructural study of the hemocytes of the pericardial body in the ascidian *Ciona intestinalis* (L.). Acta Zool. 77, 283-286.

Smith, M.J., 1970a. The blood cells and tunic of the ascidian *Halocynthia aurantium* (Pallas). I. Hematology, tunic morphology, and partition of cells between blood and tunic. Biol. Bull. 138, 354-78.

Smith, M.J., 1970b. The blood cells and tunic of the ascidian *Halocynthia aurantium* (Pallas). II. The histochemistry of blood cells and tunic. Biol. Bull. 138, 379-88.

Smith, V.J., 1981. The echinoderms, in: Ratcliffe, N.A., Rowley, A.F. (Eds.), Invertebrate Blood Cells, vol. 2, Academic Press, London, pp. 513-562.

Sugino, Y.M., Tsuji, Y., Kawamura, K., 1993. An ultrastructural study of blood cells in the ascidian *Polyandrocarpa misakiensis*: their classification and behavioral characteristics. Mem. Fac. Sci. Kochi Univ. Series D (Biology) 14, 33-41.

Sugumaran, M., Robinson, W.E., 2012. Structure, biosynthesis and possible function of tunichromes and related compounds. Comp. Biochem. Physiol. 163B, 1-25.

Vizzini, A., Parrinello, D., Sanfratello, M.A., Mangano, V., Parrinello, N., Cammarata, M., 2013. *Ciona intestinalis* peroxinectin is a novel component of the peroxidase-cyclooxygenase superfamily upregulated by LPS. Dev. Comp. Immunol. 41, 59-67.

Vizzini, A., Bonura, A., Longo, V., Sanfratello, M.A., Parrinello, D., Cammarata, M., Colombo, P., 2015. Isolation of a novel LPS-induced component of the ML superfamily in *Ciona intestinalis*. Dev. Comp. Immunol. 53, 70-78.

Vizzini, A., Di Falco, F., Parrinello, D., Sanfratello, M.A., Cammarata, M., 2016. Tranforming growth factor β (CiTGF-β) gene expression is induced in the inflammatory reaction of *Ciona intestinalis*. Dev. Comp. Immunol. 55, 102-110.

Voskoboynik, A., Soen, Y., Rinkevich, Y., Rosner, A., Ueno, H., Reshef, R., Ishizuka, K.J., Palmeri, K.J., Moiseeva, E., Rinkevich, B., Weissman, I.L., 2008. Identification of the endostyle as a stem cell niche in a colonial chordate. Cell Stem Cell 3, 456-464.

Yamaguchi, N., Amakawa, Y., Yamada, H., Ueki, T., Michibata, H., 2006. Localization of vanabins, vanadium-binding proteins, in the blood cells of the vanadium-rich ascidian, *Ascidia sydneiensis samea*. Zool. Sci. 23, 909-915.

Wright, R.K., 1981. Urochordates, in: Ratcliffe, N.A., Rowley, A.F. (Eds.), Invertebrate Blood Cells, vol. 2. Academic Press, New York, pp. 565-626.

Wright, R.K., Ermak, T.H., 1982. cellular defence systems of the protochordata, in: Cohen, N.A., Sigel, M.M. (Eds.) The Reticuloendothelial System: A Comprehensive Treatise, vol. 3, Plenum Pless, New York, pp. 283-320.

Zhang, H., Sawada, T., Cooper, E.L., Tomonaga, S., 1992. Electron microscopic analysis of tunicate (*Halocynthia roretzi*) hemocytes. Zool. Sci. 9, 551-562.

Figure legends

Fig. 1 Colony of *Diplosoma listerianum*. **A** Detail of zooids embedded in the common tunic. Scale bar: 0.5 mm. **B** Diagram of a colony section showing a single zooid exhibiting upper and lower attachment to the tunic (*dark yellow*), the common cloacal cavity (*pale yellow*) and a cloacal opening

Fig. 2 Haemoblasts of *Diplosoma listerianum*. **A** A living cell with a high nucleocytoplasmic ratio, a nucleolus and clear cytoplasm. **B-D** Histochemical characterisation of fixed haemocytes under LM. A cluster of haemoblasts stained with toluidine blue (**B**) and a single haemoblast stained using Giemsa dye (**C**) and the PAS reaction for polysaccharides (**D**). **E** TEM micrograph of a haemoblast in bloodstream. Note the evident nucleolus and the scant cytoplasmic organelles typical of a stem cell. Labels: mt, mitochondrion; N, nucleus; n, nucleolus; RER, cisternae of rough endoplasmic reticulum; v, vesicle. Scale bars: **A-D** = 2.5 µm; **E** = 2 µm

Fig. 3 Hyaline amoebocytes of *Diplosoma listerianum*. **A** A living cell with an amoeboid shape due to the presence of various pseudopodia, characterised by an ovoidal central nucleus without a nucleolus and clear cytoplasm with scant small granules. **B-E** Histochemical characterisation of fixed haemocytes under LM. Giemsa dye (**B**), PAS reaction for polysaccharides (**C**), and histoenzymatic staining for alkaline phosphatase (**D**) and β-glucuronidase (**E**). **F** Hyaline amoebocyte stained with Giemsa dye, showing an ingested yeast cell (*arrow*) as test particle in a phagocytosis assay conducted *in vitro*. **G-H** TEM micrographs of hyaline amoebocytes in the bloodstream, exhibiting cytoplasmic protrusions and cytoplasm rich in small clear vesicles as well as some phagosomes containing heterophagic electron-dense material and membrane-bound roundish granules (the homogeneous contents of which are shown in detail in the inset in **H**). Labels: g, granule, Ld, lipid droplet, mt, mitochondrion; N, nucleus; Ph, phagosome; RER, cisternae of rough endoplasmic reticulum; v, vesicle. Scale bars: **A-F** = 3.5 µm; **G-H** = 2 µm, Inset = 0.4 µm

Fig. 4 Macrophage-like cells of *Diplosoma listerianum*. **A** A living cell with the nucleus displaced at the periphery due to the presence of large phagosomes. **B-D** Histochemical characterisation of fixed haemocytes under LM. Giemsa dye showing metachromatic

staining of the phagosome contents (**B**) and histoenzymatic staining for alkaline phosphatase (**C**) and β-glucuronidase in vacuolar contents (**D**). **E** A macrophage-like cell stained with Giemsa dye containing engulfed yeast cells (*arrows*) at various degrees of digestion inside the heterophagic vacuoles. **F** TEM micrograph of macrophage-like cells in the bloodstream, showing an ingested cell in its large phagosome, delimited by a peripheral ring of cytoplasm containing numerous clear vesicles. Labels: mt, mitochondrion; Ph, phagosome; RER, cisternae of rough endoplasmic reticulum; v, vesicle. Scale bars: **A-E** = 4 μm; **F** = 2 μm

Fig. 5 Granular amoebocytes of *Diplosoma listerianum*. **A.** A living cell with an amoeboid shape, exhibiting a central nucleus and cytoplasm rich in large pale-yellow granules. **B-D** Histochemical characterisation of fixed haemocytes under LM. Giemsa dye showing metachromatic granules (**B**), the PAS reaction (**C**), and histoenzymatic staining for phenoloxidase (**D**). **E-H** TEM micrographs of granular amoebocytes in the bloodstream, exhibiting cytoplasmic protrusions and a nucleus without a nucleolus (**E**), vesicles interspersed in the cytoplasm, small membrane-bound granules with homogeneous content (**F** as detail of **E**, and **G**) and large granules containing highly electron-dense material, probably consisting of osmiophilic polyphenols and phenoloxidase, at various degrees of organisation and attached to the membrane facing the granule (**F**,**H**). Labels: G, Golgi apparatus; g, granule; mt, mitochondrion; N, nucleus; PO-g, phenoloxidase-containing granule; v, vesicle. Scale bars: **A-D** = 4.2 μm; **E** = 2 μm; **F-H** = 0.5 μm

Fig. 6 Morula cells of *Diplosoma listerianum*. **A** A living cell with cytoplasm filled with large, pale-yellow granules. **B** Blue autofluorescence of granules under UV light in an aldehyde-fixed cell. **C-I** Histochemical characterisation of fixed haemocytes under LM. Metachromatic staining of granules with Giemsa dye (**C**), staining based on the tintorial affinity for eosin dye (**D**), staining via the PAS reaction (**E**), polyphenol staining via Masson-Fontana's argyrophil reaction (**F**), weak MBTH staining for quinones (**G**), and histoenzymatic staining for alkaline phosphatase (**H**) and phenoloxidase (**I**). **J-K** TEM micrographs of morula cells in the bloodstream, showing roundish nuclei, sometimes containing a nucleolus, and cytoplasm with cisternae of rough endoplasmic reticulum and numerous large osmiophilic granules, containing polyphenols and phenoloxidase, and smaller membrane-bound granules, with homogeneous contents. Labels: G, Golgi apparatus; g, granule; mt, mitochondrion; N, nucleus; n, nucleolus; PO-g, phenoloxidase-

containing granule; RER, cisternae of rough endoplasmic reticulum. Scale bars: **A-I** = 4.5 µm; **J** = 2 µm; **K** = 0.5 µm

Fig. 7 Morula cell morphology after an immune stimulus causing degranulation. **A** A living cell. Note the smaller number of granules in the cytoplasm, which are mainly displaced at the periphery. **B** Dark red MBTH staining of residual granules, indicating extensive production of quinones from the oxidation of polyphenols by activated phenoloxidase. **C-D** TEM micrographs of degranulating morula cells in the bloodstream, showing the process involving the large osmiophilic granules. **E-F** Details of the large osmiophilic granules in **C** and **D**, which are partially fused together, showing the electron-dense contents concentrated in the centre of the granules (**E**) and attached to the membrane of the almost completely empty granules as residual material (**F**). Labels: g, granule; PO-g, phenoloxidase-containing granule; RER, cisternae of rough endoplasmic reticulum. Scale bars: **A-B** = 4.5 µm; **C-D** = 2.5 µm; **E-F** = 1 µm

Fig. 8 Mast cell-like granulocytes of *Diplosoma listerianum*. **A** A living cell with cytoplasm filled with clear granules, displacing the roundish nucleus at the periphery. **B-E** Histochemical characterisation of fixed haemocytes under LM. Giemsa dye (**B**), PAS reaction for polysaccharides (**C**), basophilic (green) staining with Ehrlich's mixture (**D**), and Csaba's reaction for the identification of high-sulphated heparin (magenta) and weakly or non-sulphated glucosaminoglycans (blue) (**E**). **F-G** Immunocytochemistry for the co-localisation of histamine (**F**) and heparin (**G**) in granules within the same cell. DAPI counterstaining for nuclei. Note that histamine is concentrated at the centre and heparin at the periphery leaning against the membrane of the granules. **H** A living cell showing characteristics of degranulation after incubation with compound 48/80. **I** Cell recognised by ConA. **J-K** TEM micrographs of mast cell-like granulocytes in the bloodstream (**J**) and details of their granules (**K**), showing an electron-dense core. Labels: N, nucleus. Scale bars: **A-I** = 4.5 µm; **J** = 2.5 µm; **K** = 0.5 µm

Fig. 9 Spherule cells of *Diplosoma listerianum*. **A** A living cell showing a globular shape, exhibiting large vacuoles filled with minute granulations and displacement of the nucleus to the periphery. **B** Histochemical characterisation of fixed haemocytes under LM showing positivity for the PAS reaction. **C-F** TEM micrographs of spherule cells in the bloodstream. The nucleus contains an evident nucleolus (**C**,**E**). In detail, the Golgi apparatus is very

developed in the centre of the cell, with its cisternae forming a honeycomb structure (**F**), and the clear granules contain filamentous material (**D**). Labels: G, Golgi apparatus; g, granule; N, nucleus; n, nucleolus. Scale bars: **C-D** = 1 μm; **E** = 2 μm; **F** = 0.5 μm

Fig. 10 Nephrocytes of *Diplosoma listerianum*. **A** A living cell observed with 45°-incident light to show the birefringence of vacuolar inclusions. **B-D** TEM micrographs of nephrocytes in the bloodstream. The nucleus and Golgi apparatus are evident, together with numerous mitochondria (**B**). Vacuolar inclusions appear as parallel chains (**C**, showing a detail of **B**) or hexagonal structures (**D**) depending on sectioning plane. Labels: G, Golgi apparatus; mt, mitochondrion; N, nucleus. Scale bars: **A** = 2.3 μm; **B** = 1.5 μm; **C** = 0.2 μm; **D** = 0.16 μm

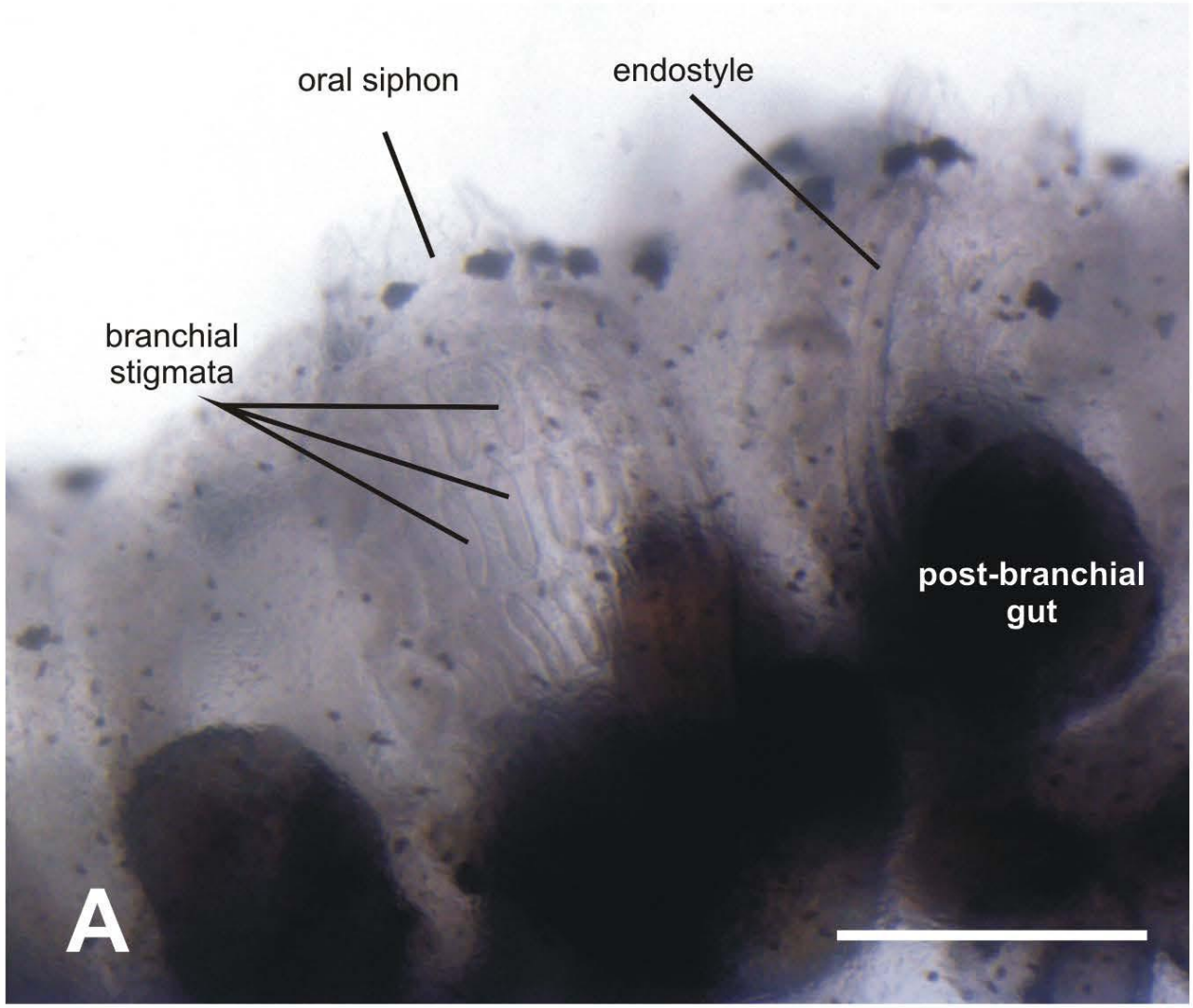
oral siphon
endostyle
branchial stigmata
post-branchial gut
A

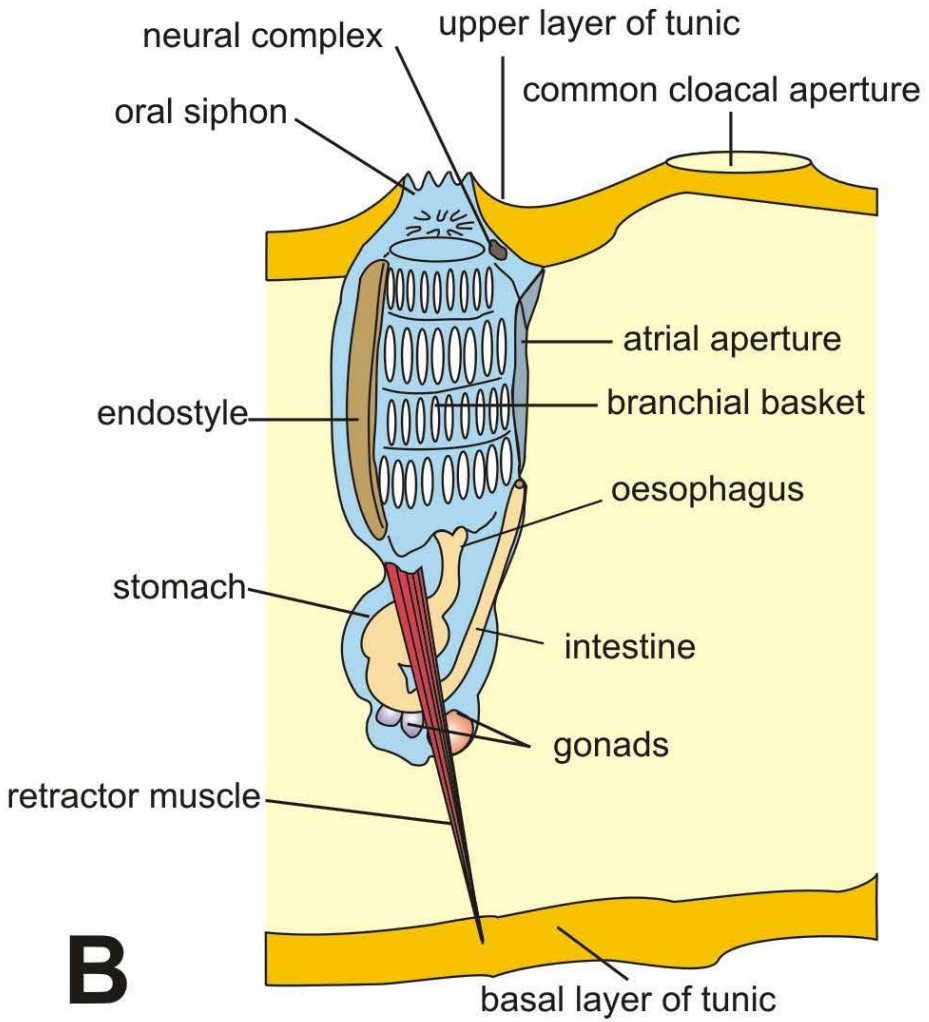
neural complex
upper layer of tunic
common cloacal aperture
oral siphon
atrial aperture
branchial basket
endostyle
oesophagus
stomach
intestine
gonads
retractor muscle
basal layer of tunic
B

Fig. 1

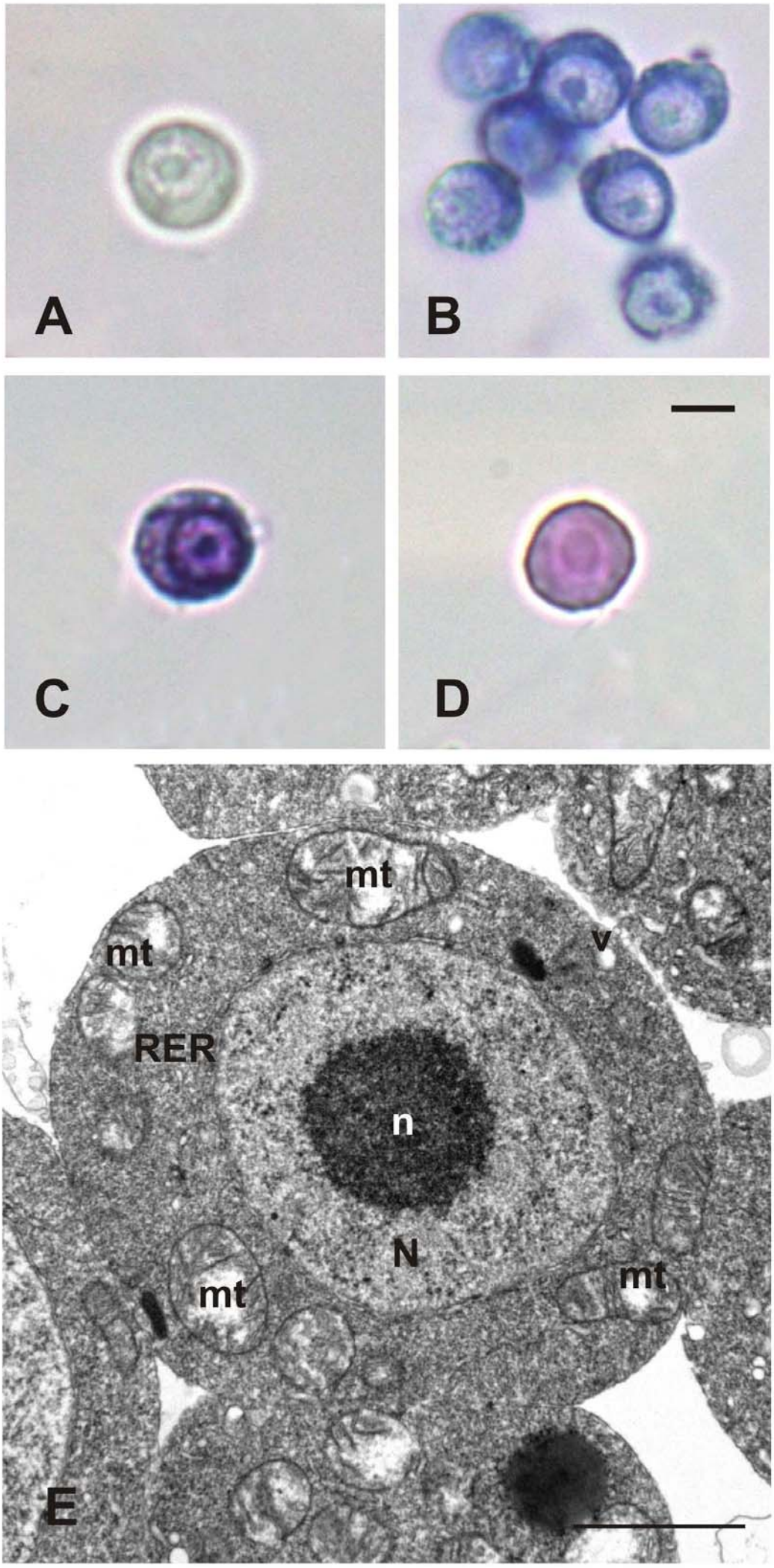

Fig. 2

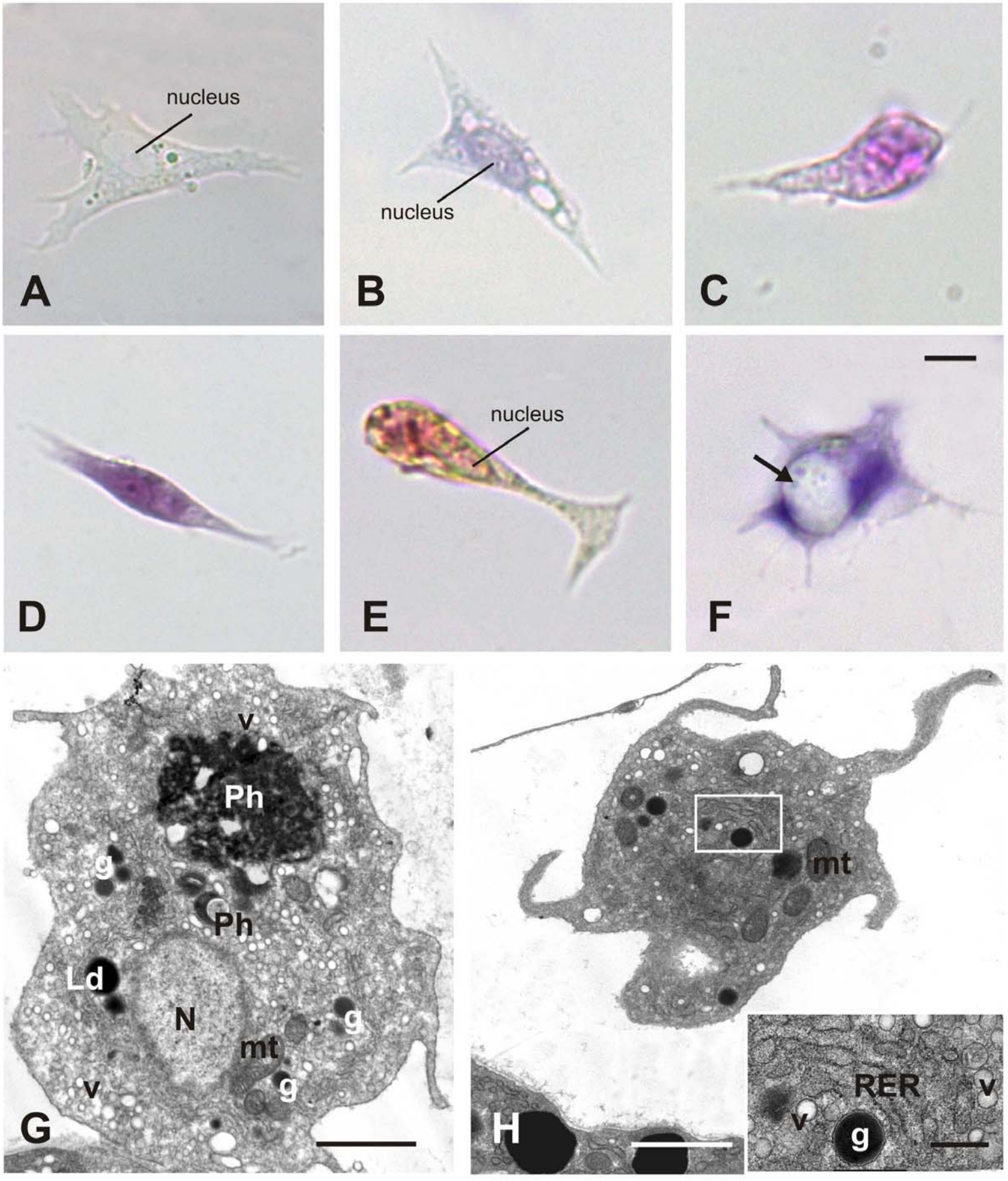
nucleus
A
nucleus
B
C
D
nucleus
E
F
v
Ph
g
Ph
Ld
N
g
mt
v
g
G
mt
H
RER
v
v
g

Fig. 3

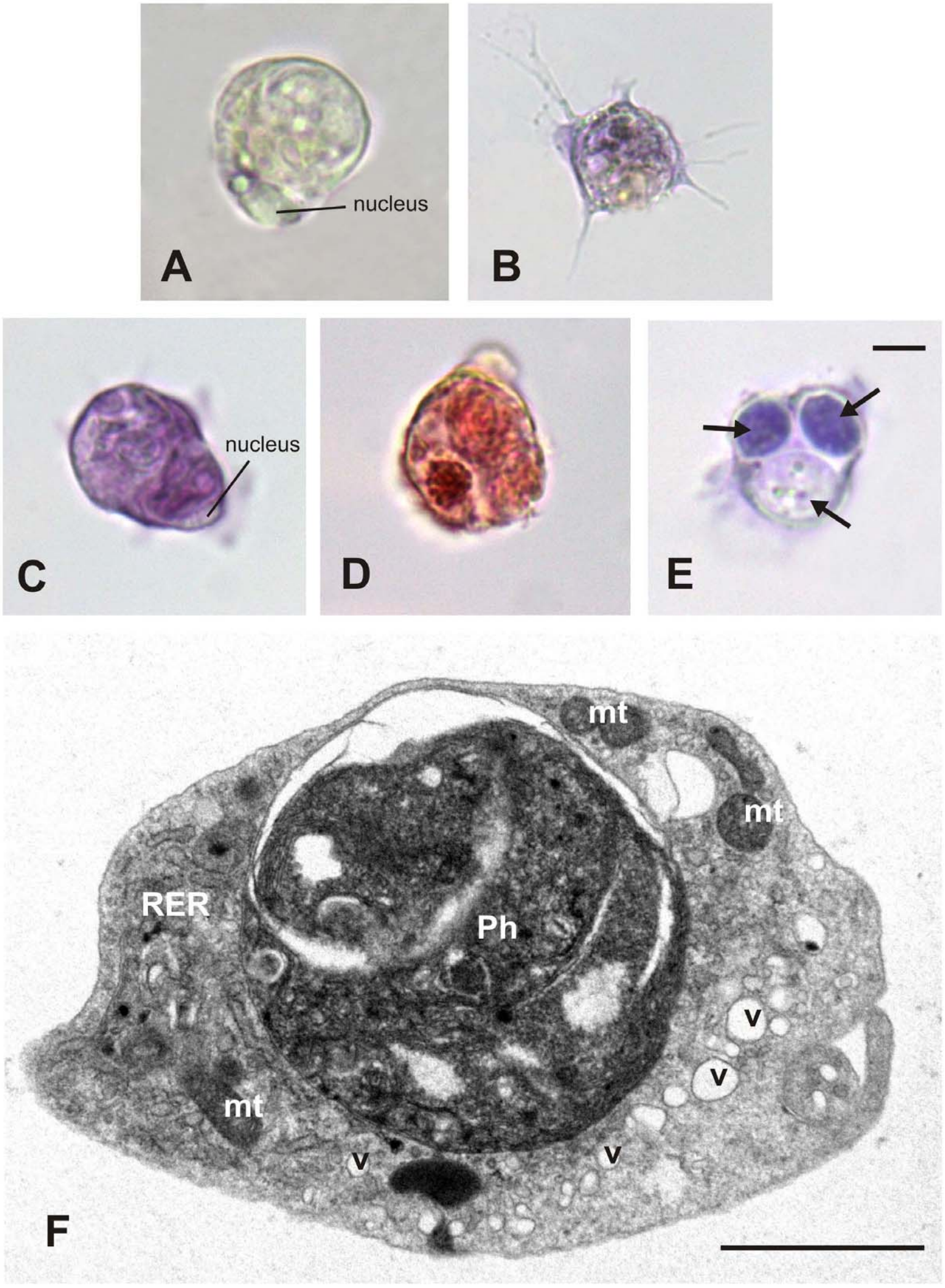

Fig. 4

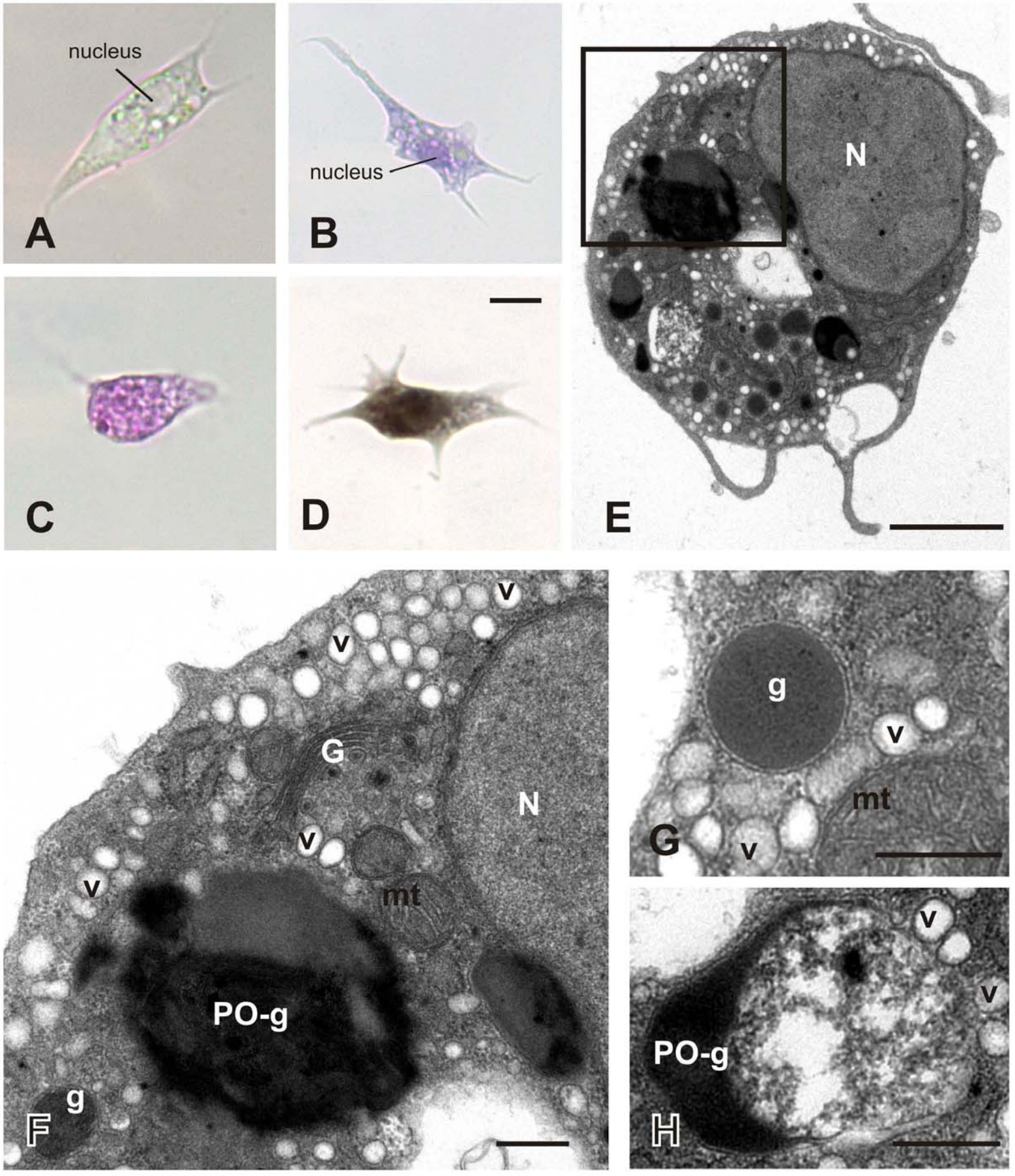

Fig. 5

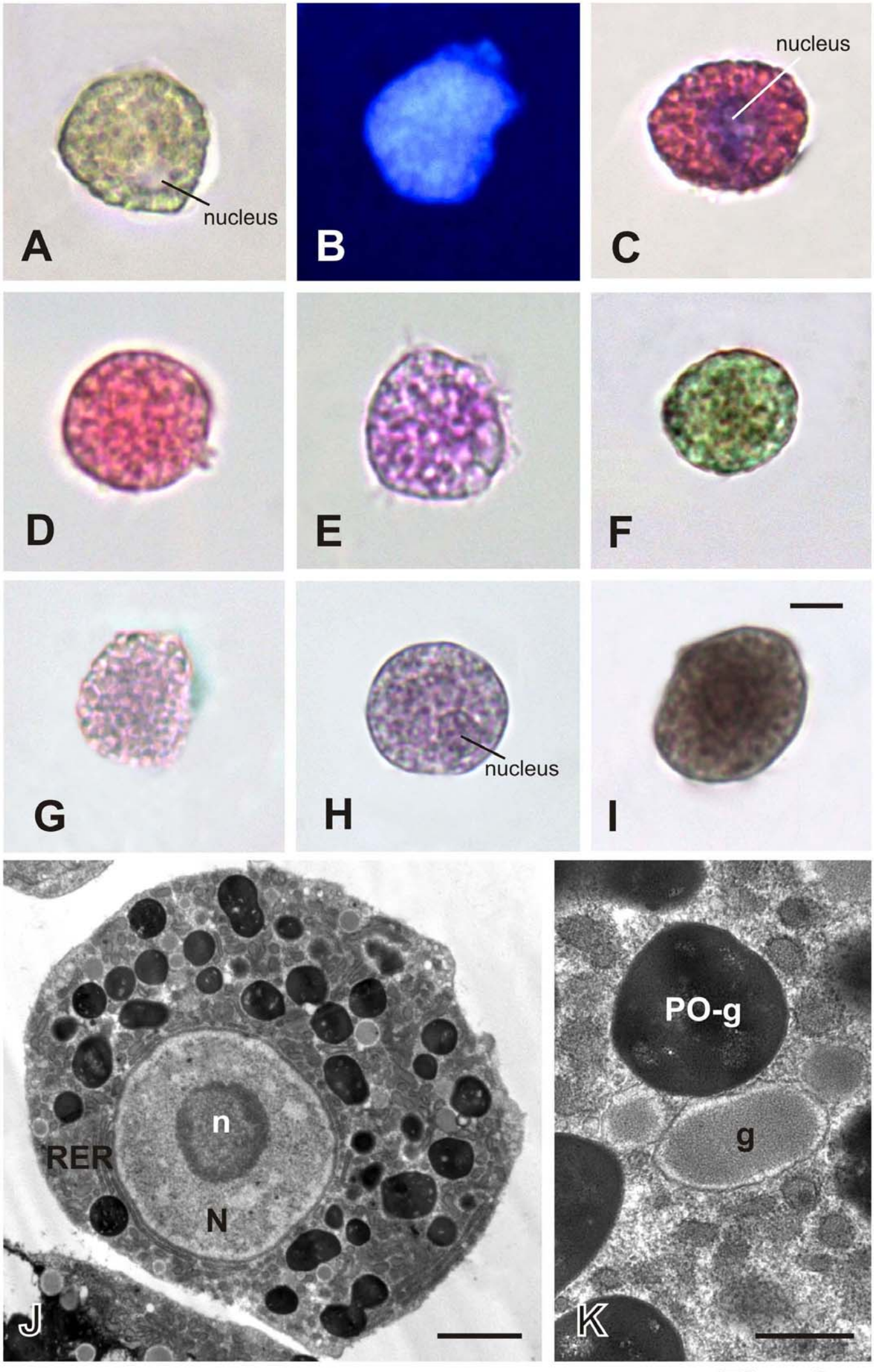

Fig. 6

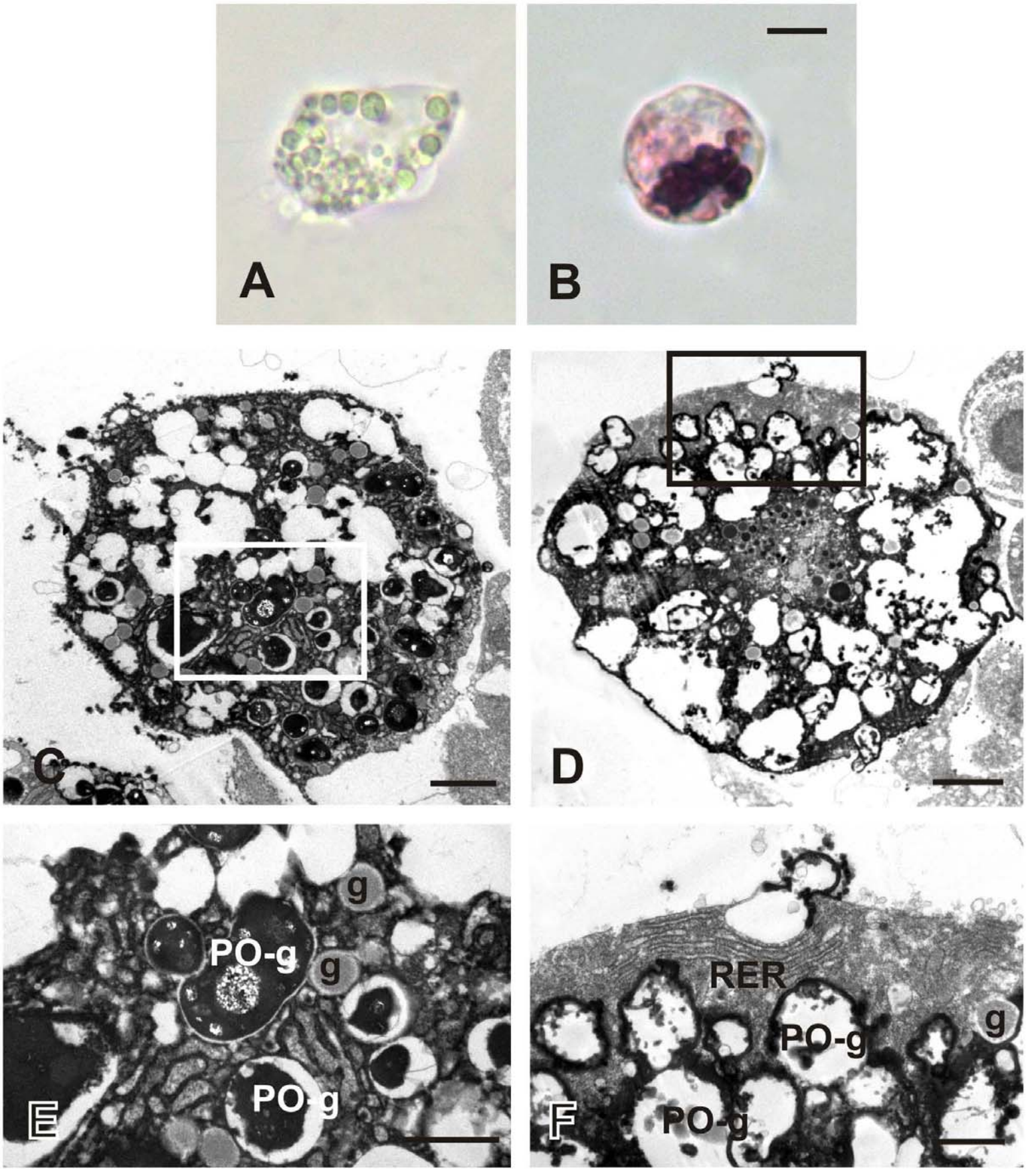

Fig. 7

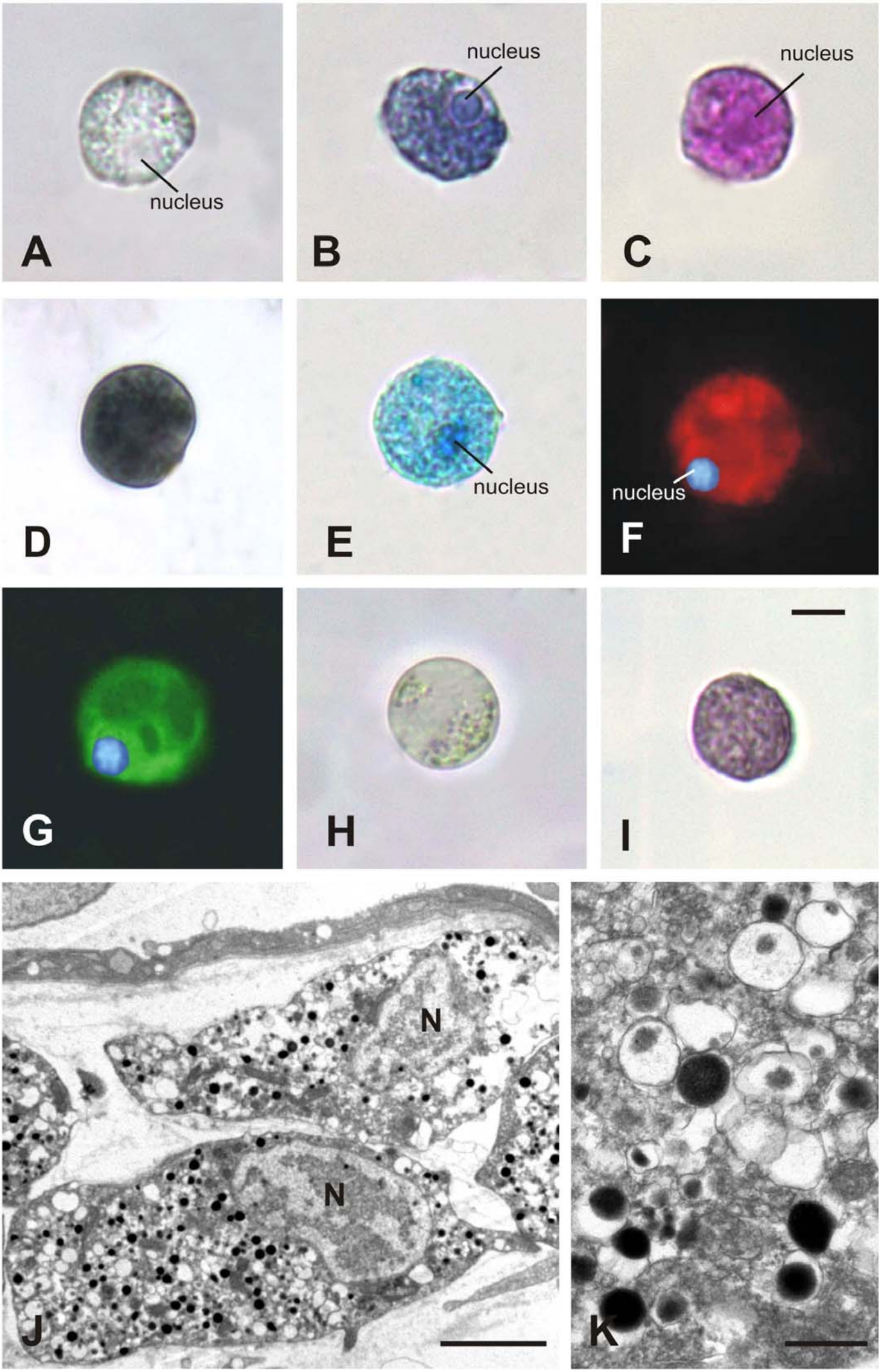

Fig. 8

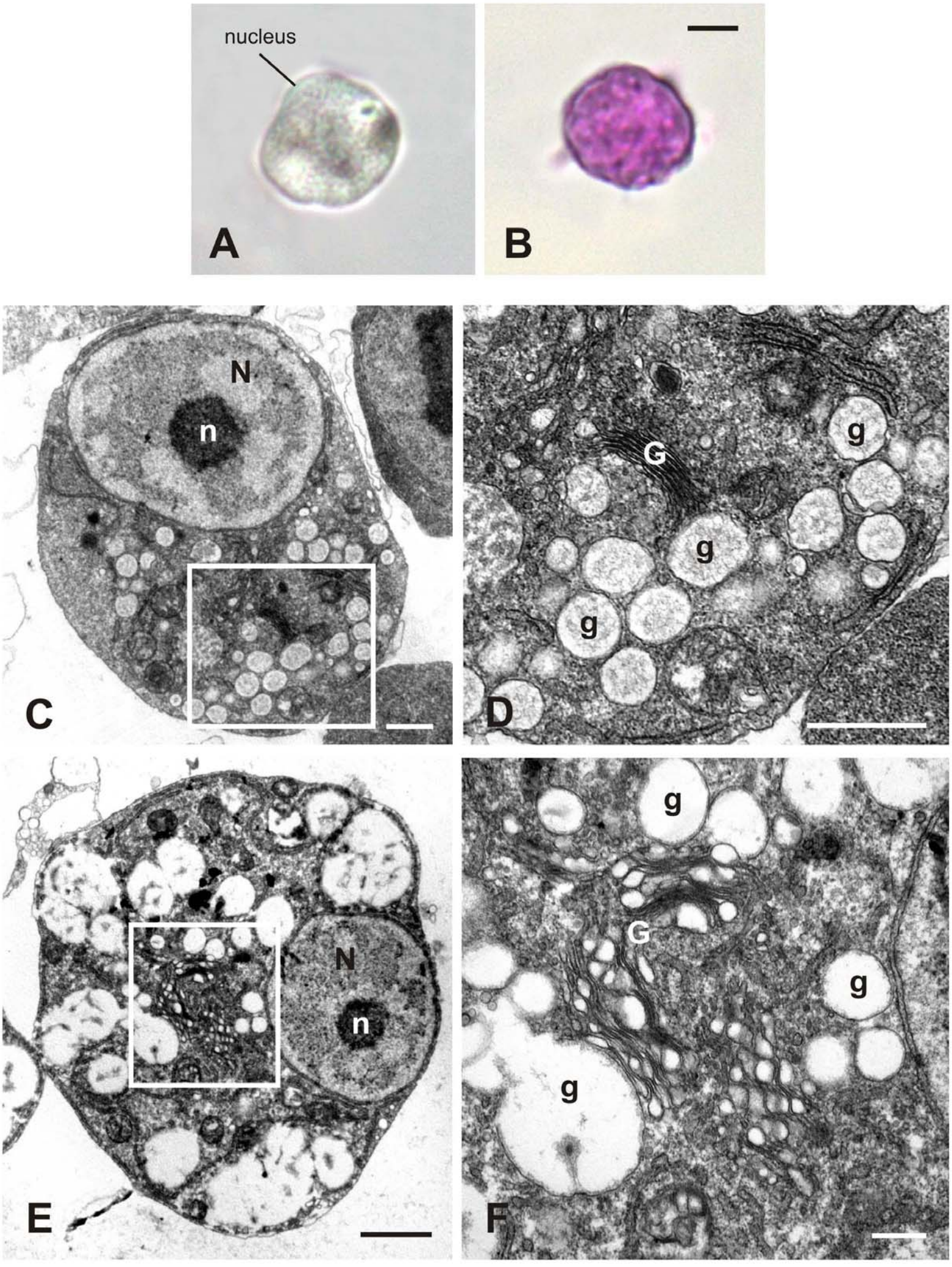

Fig. 9

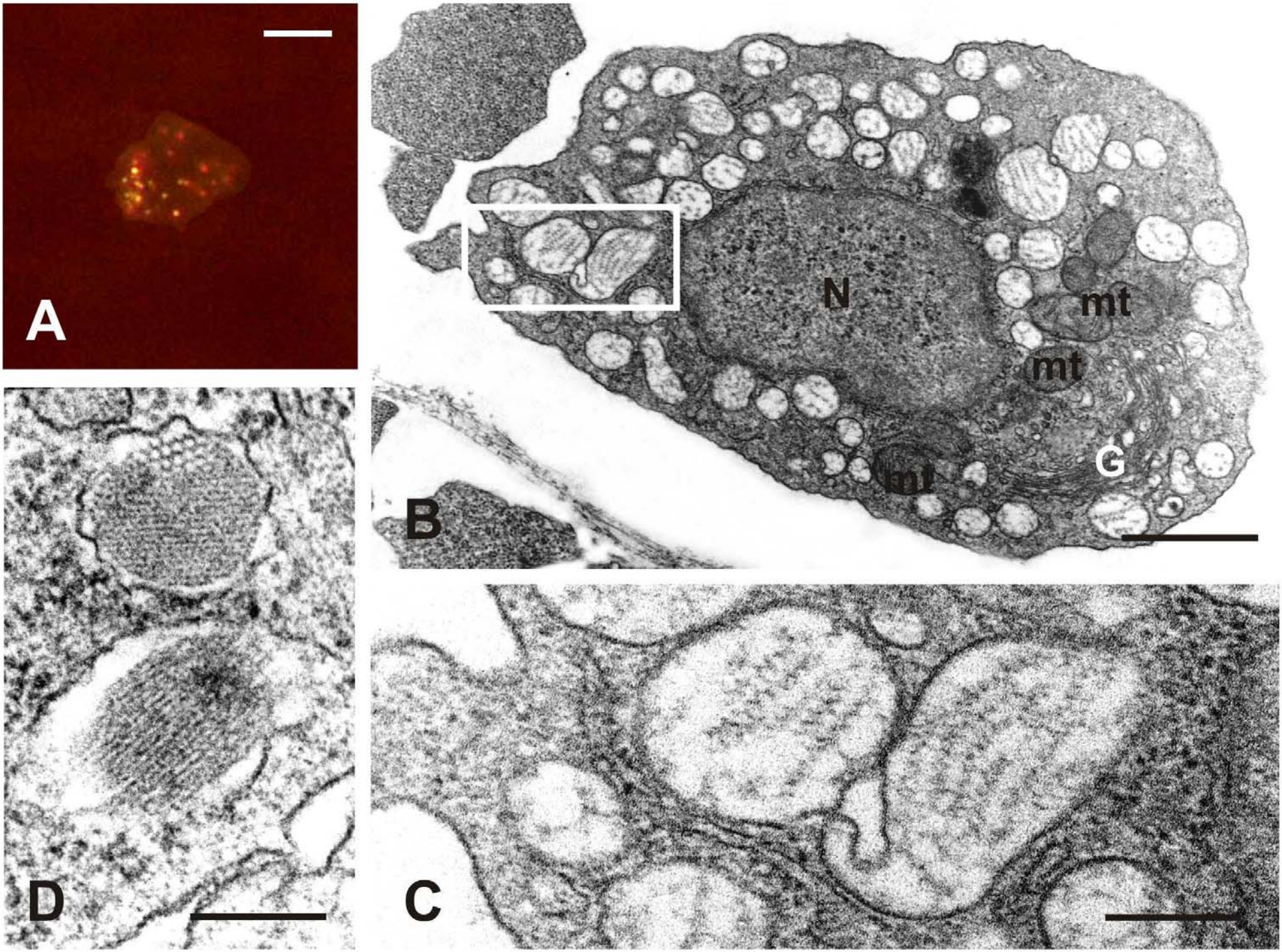

Fig. 10

Table 1 Histochemical properties, enzymatic activity and lectin affinity of *Diplosoma listerianum* haemocytes

	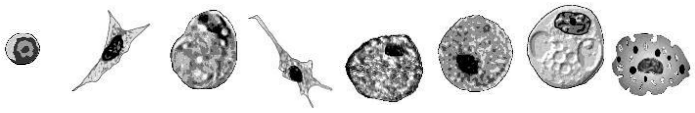							
	H	HA	MPL	GA	MC	MLG	SC	N
HISTOCHEMICAL ASSAYS								
Toluidine blue	+	+	+	+	+	+	+	+
Giemsa's dye	+	+	+	+	+	+	+	+
Eosin dye			+	+	+			
Ehrlich's mixture			+	+	+	+		
PAS reaction	+	+	+	+	+	+	+	
Masson-Fontana's reaction				+	+			
MBTH staining				+	+			
Csaba's mixture						+		
LECTIN AFFINITY								
Narcissus pseudonarcissus agglutinin (NPA)						+		
Concanavalin A (ConA)						+		
HISTOENZYMATIC ASSAYS								
a) *Hydrolytic enzymes*								
Alkaline phosphatase	+	+	+		+			
ß-glucuronidase		+	+					
b) *Oxidative enzymes*								
Phenoloxidase				+	+			
IMMUNOHISTOCHEMICAL ASSAYS								
Anti-heparin						+		
Anti-histamine						+		

H: haemoblast; HA: hyaline amoebocyte; MPL: macrophage-like cell; GA: granular amoebocyte; MC: morula cell; MLG: mast cell-like granulocyte; SC: spherule cell; N: nephrocyte

Table 2 Comparative classification of corresponding haemocyte morphotypes in tunicates

Ascidiacea Stolidobranchia	Ascidiacea Phlebobranchia	Ascidiacea Aplousobranchia	Thaliacea Salpida
Haemoblast*, Stem cell*, Undifferentiated cell*	Haemoblast*, Stem cell*	Haemoblast[1]	Haemoblast[2], Undifferentiated cell[2]
Hyaline amoebocyte[3,4,5], Microgranular amoebocyte[3], Hyaline cell[6]	Non-vacuolar hyaline amoebocyte[7], Clear vesicular granulocyte[7]	Hyaline amoebocyte[1]	Hyaline amoebocyte[2]
Macrophage-like cell[3,4,5], Phagocyte[6,8]	Vacuolar hyaline amoebocyte[7,9], Phagocyte[7,9]	Macrophage-like cell[1]	Amoebocyte with large vacuoles[2]
Granular amoebocyte[3,4], Macrogranular amoebocyte[3]	Granular amoebocyte[7], Microgranulocyte[7]	Granular amoebocyte[1]	—
Morula cell[3,4,5]	Morula cell[7,9], Globular granulocyte[7,9]	Morula cell[1]	—
—	Univacuolar refringent granulocyte[7], Unilocular granulocyte[7], Univacuolar refractile granulocyte[9]	—	—
—	Vanadocyte[7,9,10], Signet-ring cell[7,9,10]	—	—
Compartment cell[4], Compartment amoebocyte[4], Macrogranular leukocyte[5,11], Trophocyte[5,11]	Compartment cell[7,9]	—	—
Basophilic granulocyte[4,6,8], Granular cell[4,6,8]	Basophil granulocyte[7,10] Cell with acidic vacuoles[9]	Mast cell-like granulocyte[1]	Granular cell[2]
Giant cell[8], Glomerulocyte[5]	Globular granulocyte[7]	Spherule cell[1]	—
Nephrocyte[3,4]	Nephrocyte[9,12]	Nephrocyte[1]	Nephrocyte[2]
Pigment cell[3,4,5]	Pigment cell[9], Orange cell[7]	—	—

*All genera, [1]*Diplosoma*, [2]*Thalia*, [3]*Botryllus*, [4]*Botrylloides*, [5]*Polyandrocarpa*, [6]*Styela*, [7]*Ciona*, [8]*Halocynthia*, [9]*Phallusia*, [10]*Ascidia*, [11]*Polyzoa*, [12]*Ascidiella*